University of South-Eastern Norway

www.usn.no

FMH606 Master's Thesis 2018

Process Technology

Computational modeling and experimental studies on fluidized bed regimes

Rajan Jaiswal

Faculty of Technology, Natural sciences and Maritime Sciences

Campus Porsgrunn

University of South-Eastern Norway

www.usn.no

Course: FMH606 Master's Thesis, 2018

Title: Computational modeling and experimental studies on fluidized bed regimes

Number of pages: 52

Keywords: Fluidized bed, pressure drop, superficial gas velocity, regimes, static bed height, particle size distribution, density, CPFD

Student: Rajan Jaiswal

Supervisor: Prof. Britt Margrethe Emilie Moldestad, Cornelius Emeka Agu

Availability: Open

Faculty of Technology, Natural sciences and Maritime Sciences
Campus Porsgrunn

University of South-Eastern Norway

www.usn.no

Summary:

The fluidization technology has a wide range of applications from chemical synthesis to pneumatic transportation and circulation of species. Different process applications require different flow regimes and the type of flow regimes depends on superficial gas velocity, particle size distribution, particle density and reactor dimensions.

This study investigates the influence of initial bed height, particle density and particle size distribution on the fluidized bed regime transition. Experiments are performed on a cold bed with sand, limestone and glass beads particles as bed materials. A Computational Particle Fluid Dynamic (CPFD) model is established using Wen- Yu and Ergun drag model in a simulation software Barracuda VR and further the CPFD model is validated using experimental results. The results from the simulations are compared with the experimental data and correlations in the literature. The onset of each regime i.e. minimum fluidization, bubbling, slugging and turbulent regime is identified using statistical analysis techniques. The statistical analysis methods include standard deviation of pressure fluctuation along the height of the bed and the change in solid volume fraction in the bed as a function of gas velocity.

The results show that the minimum fluidization velocity for sand ($d_m = 234\mu m$) and limestone remain constant with change in the aspect ratio while it decreases to a stable value below aspect ratio of 1.5 for sand particle with mean diameter ($d_m = 346\mu m$). Similarly, the minimum bubbling velocity for all the three types of particles are found to be independent of the static bed height. The onset of slugging velocity decreases with increase in the bed height for all the three particle types. The turbulent velocity for sand particles ($d_m = 234\mu m$) increases slightly with increase in aspect ratio while it almost remains constant for sand ($d_m = 346\mu m$) and limestone. With the increase in particle size distribution for limestone, $400\mu m - 1400\mu m$, there is significant increment in minimum fluidization, bubbling, slugging and turbulent velocity.

Faculty of Technology, Natural sciences and Maritime Sciences

Campus Porsgrunn

Acknowledgements

I would especially like to thank my supervisor prof. Britt Margrethe Emilie Moldestad for her continuous support and guidance. Her clear explanations on the subject has enabled me to learn the fundamentals within a short span of time. In addition to the academic knowledge, I learned some valuable traits, during this period, which I believe will be useful for me throughout my life. She has been "a Guru (गुरु)"- an inspirational source to me.

I would like to thank my co-supervisor Cornelius Emeka Agu for his advice, explanation, and encouragement. Also, allowing me to reach him anytime for discussion.

Special thanks to Rajan Kumar Thapa for his advice and care. During this entire period of studies at USN, he has been like a parent to me. It is not possible to explain in words the support and care I received from him.

Thanks to Janitha Bandara for helping me with the simulations. It would really have been difficult with his support.

Thanks to my friend Om Prakash chapagain for helping me with the MATLAB coding, it would have been time consuming and difficult without his help.

Last but the most important, without nothing would have been possible. Thanks to USN(Porsgrunn) management and administration for providing immense facilities. As an International student, I felt like a home at USN.

Porsgrunn, 24/05/2018

Rajan

Abstract

The fluidization technology has a wide range of applications from chemical synthesis to pneumatic transportation and circulation of species. Each process applications require different flow regimes and the type of flow regimes depends on superficial gas velocity, particle size distribution, particle density and reactor dimensions.

This study investigates the influence of initial bed height, particle density and particle size distribution on the fluidized bed regime transition. Experiments are performed on a 3D cold fluidized bed with sand, limestone and glass bead particles as bed materials. A Computational Particle Fluid Dynamic (CPFD) model is established in simulation software Barracuda VR using Wen- Yu and Ergun drag model and further the CPFD model is validated using experimental results. The results from the simulations are compared with the experimental data and correlations in the literature. The simulation results show good agreement with the experimental data. Each regime i.e. minimum fluidization, bubbling, slugging and turbulent regime is identified using pressure and solid volume fraction fluctuation during fluidization as a function of superficial gas velocity.

The result shows that the minimum fluidization velocity for sand ($d_m = 234\mu m$) and limestone remain constant with change in aspect ratio while it decreases to a stable value below aspect ratio 1.5 for sand particle with mean diameter ($d_m = 346\mu m$). Similarly, the minimum bubbling velocity for all three particles are found to be independent of static bed height. The onset of slugging velocity decreases with increase in bed height for all three particles. The turbulent velocity for sand particles ($d_m = 234\mu m$) increase slightly with increase in aspect ratio while it almost remains constant for sand ($d_m = 346\mu m$) and limestone.

With the change in particle size distribution from $100 - 200\,\mu m$ to $200 - 400\mu m$ for sand particles there is increment in minimum fluidization, minimum bubbling, slugging and turbulent velocity. Similarly, in case of limestone with particle size distribution of $400 - 1400\mu m$, there is significant increment in superficial gas velocity at which different regime is established compared to that of sand particles.

Contents

Nomenclature

Symbol	Description	SI units
U_{mf}	Minimum fluidization velocity	m/s
U_{mb}	Minimum bubbling velocity	m/s
U_c	Critical velocity	m/s
σ	Standard deviation	*pascal*
$\overline{P}$	Mean pressure	*pascal*
N	Number of data sets	-
H, h_0	Static bed height	m
D	Diameter of the column	m
ΔP_b	Pressure drop across the bed	*pascal*
A_t	Cross section area of the bed	m^2
L_{mf}	Bed at minimum fluidization	m
$\varepsilon_m, \varepsilon_{mf}$	Void fraction in a fixed bed, in a bed at minimum fluidization condition	-
ρ_g, ρ_s	Gas density, density of solid	kg/m^3
g_c, g	Conversion factor, acceleration due to gravity	$\left[\frac{9.8kg.m}{kg-w.s^2}\right], m/s^2$
μ	Viscosity of gas	$kg/m.s$
ϕ_s	Sphericity of particle	-
d_p, d_m	Particle mean diameter	m

Ar	Archimedes Number	-
Re_p	Particle Reynolds number	-
ψ	ratio of observed bubble flow	-
u_b, u_{br}, u_0	Velocity of bubble rise through a bed, rise velocity of bubble with respect to emulsion phase, superficial gas velocity	m/s
d_b	Effective bubble diameter	m
$U_{S\infty}, U_S$	Rise velocity of square nosed slugs rise velocity of a single axisymmetric slug	m/s
U_{bs}	Minimum slugging velocity (Bubble to slug transition)	m/s
a, c	Fitting index, fitting coefficient	-
t, s, b (subscripts)	Transition, solid, bubble	-
w_s	Solid weight fraction	-

List of figures

List of tables

1 Introduction

1.1 Background

Fluidization technology has wide range of applications in many processes like chemical synthesis, pneumatic transportation, chemical regeneration, powder mixtures and even in the hospitals[2] for example, treatment of Ulcer patients. Each application requires different flow regimes. The type of flow regime that can be established in fluidized beds depends on the parameters such as superficial gas velocity, particle properties, and bed dimensions. The properties of fluidized bed based on the parameters have been widely studied by many researchers [3-5]. However, the dynamic behaviour of the bed in different fluidization regimes, still, remain dubious.

Basically, fluidization is the process of forcing gas in the bed of solid materials and transferring the static solid particles into a suspension. At this stage, the bed exhibits properties analogous to dynamic liquid state and can extend from loose bed to pneumatic conveying depending on the inlet superficial gas velocity. The superficial gas velocity at which the frictional force between the fluid and particles are counterbalance by the weight of the bed is said to be minimum fluidization velocity (u_{mf}) and the pressure drop due to weight of the bed at this point is the maximum pressure drop [1]. With the increase in gas velocity, bubbles start to form and rise in the bed depending on the properties of the particles. For a bed with smaller particles, the bed expands significantly before there is formation of bubbles[6] while, for a bed with larger particle diameters (Geldart B particle), the bubbles start to form as soon as the bed is fluidized. The onset of bubbling regime is said to be establish at the superficial velocity when the bubbles first appear in the bed and the corresponding velocity is called minimum bubbling velocity(u_{mb}) [7]. With Further increase in the gas velocity, the bubble diameter and bubble rise velocity increases[8]. When the bubble diameter is $\sim(0.3-0.6)D$, the bed slugs and different type of slugs axisymmetric, squared-nose and wall slug, appearing in the bed, depends on the particle type, particle size, bed diameter and the wall of the column[7, 9]. Bubble and slug flow largely influence the gas and solid interaction in the fluidized bed thus, identifying onset of bubbling and slugging regime and their transition zone is crucial for the design of fluidized bed reactors. The slug flow shifts into turbulent with further increase in gas velocity followed by random fluctuation of pressure drop. The turbulent regime is marked with the absence of bubbles and slugs in the bed and is followed by violent movement of elongated and distorted voids of particles. For a fluidized bed with small particles, an increase in superficial gas velocity beyond bubbling velocity, the fluctuation in pressure drop reaches a peak value at critical velocity (u_c), declines and reaches steady value with the increase in superficial gas velocity to u_k[10]. In the case of coarse particles, for instant Geldart D particles, large exploding bubbles are absorbed before it reaches turbulent regime. Once the turbulent regime is stablished, it is followed by severe channelling and large-scale uniform circulation of bed material termed as churning fluidization[1]. Flow regimes in fluidized bed can be established by various approaches, however, a statistical analysis method as standard deviation of pressure fluctuation is the simplest and most economical method and can be implemented without affecting the inlet gas flow[11].

In this work, the flow regimes: minimum fluidization, bubbling, slug and turbulent regimes are identified using both experimental data and Computational Particle Fluid Dynamic (CPFD) model. CPFD model was developed using CPFD software Barracuda VR. The onset and transition of the regimes have been identified for sand, limestone and glass particles with five aspect ratios using standard deviation of pressure fluctuation and fluctuation of solid volume fraction of bed materials during fluidization. The standard deviation (σ) of pressure fluctuation with change in superficial gas velocity can be calculated as in equation 2.1. The methods to established different regimes are discussed later in this work.

1.2 Objective

The primary goal of this work is to study hydrodynamic behavior of fluidized bed regimes and investigate the influence of static bed height and particle size distribution on the different fluidized bed regimes. To achieve this goal, this work accomplishes the following objectives:

1. Literature review on the influence of bed height and particle size distribution on fluidized bed regimes.
2. Short literature review on regime analysis techniques
3. Experiments on a cold fluidized bed (present at USN) with four different particles using compressed air
4. Establish a valid Computational Particle Fluid Dynamic (CPFD) model.
5. Identify the fluidized bed regimes for each aspect ratio ($\frac{H}{D} = 0.7, 1, 1.5, 2, 2.5$) using statistical analysis techniques
6. Evaluate the effect of static bed height on different regimes
7. Compare the effect of material density and particle size distribution on fluidized bed regimes
8. Identify the minimum bed height at which the total bed pressure drop is the same as that due to the weight of the bed.

1.3 Overview and Scope of thesis

This work is divided into mainly four parts. First part, Chapter 2 and Chapter 3, summarizes the literature review of fluidized bed regimes and regime identification techniques. The experimental and simulation set up, equipment, bed material properties, a CPFD model are described in Chapter 4 and Chapter 5. Experimental and simulation results for each set of experiments are described in Chapter 6. Similarly, Chapter 7 presents the analysis and discussion of the experimental and simulation results under two section 7.1 and 7.2. The influence of bed height and particle size distribution are discussed is section 7.1 and section 7.2 respectively. Chapter 8 concludes the entire work. Figure 1.1 illustrates the overall procedure carried out in this work to identify different regimes.

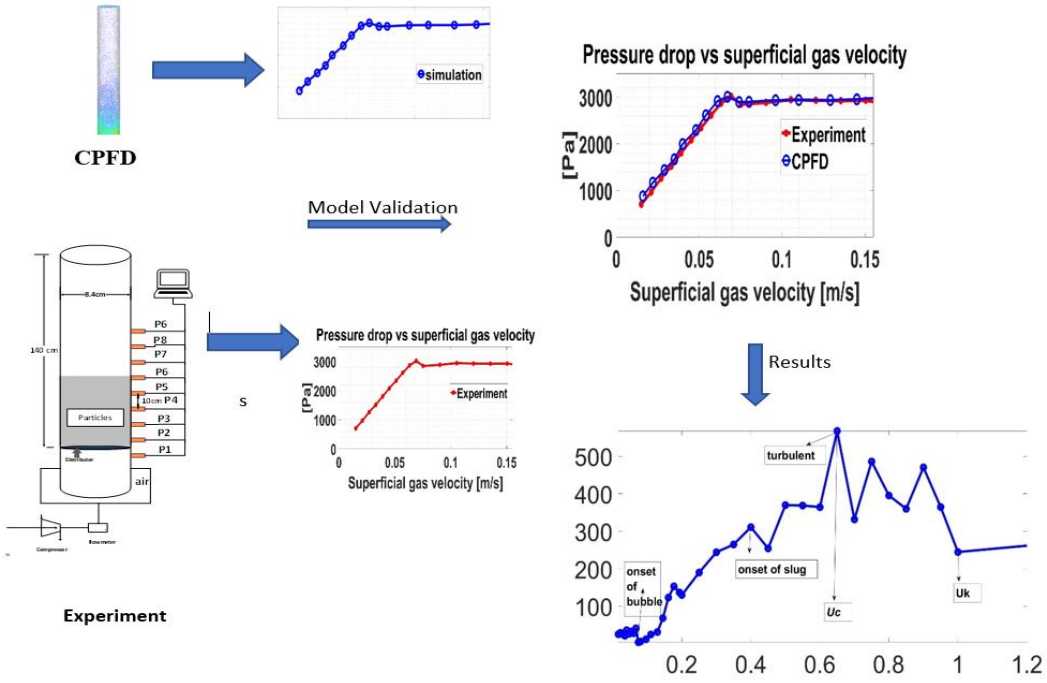

Figure 1.1: Schematic diagram showing overview of the work

2 Literature Review on Fluidization Phenomenon and Fluidization Regimes

Fluidization is the process of forcing gas into a bed of solid materials and transferring static solid particles into suspension in the gas phase. The fluidized bed exhibits properties analogous to dynamic liquid state and can extend from loose bed to pneumatic conveying depending on the inlet gas properties (superficial gas velocity), bed properties (material density, shape, size) and bed dimensions.

With the increase in superficial gas velocity, the fixed bed particles vibrate and tends to occupy restricted regions transforming the fixed bed into expanded bed. Further increase in flow rate, changes the bed regimes from minimum fluidization to pneumatic conveying as shown in *Figure 2.1*[1].

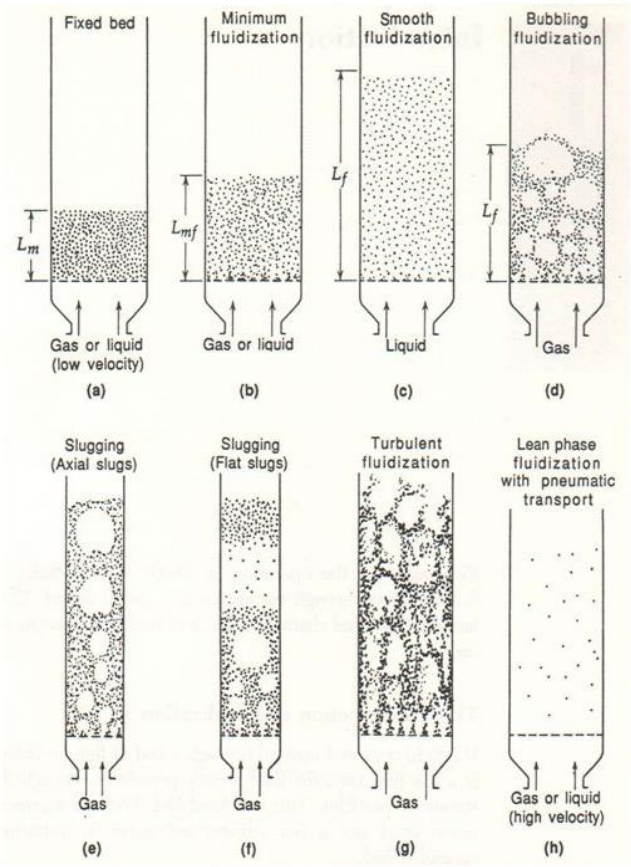

Figure 2.1:Fluidized bed regimes [1]

2.1 Minimum Fluidization

The dynamic state of expanded bed particles when it remains suspended in gas is said to be in a state of minimum fluidization or incipient fluidization. At this point, the pressure drop across the bed is equal to the total weight of the bed per unit area and the frictional force between the fluid and particles counterbalance the weight of the bed. The superficial gas velocity at this stage is called as minimum fluidization velocity (u_{mf}) where the pressure drop across the bed is maximum. This from fixed bed to fluidized bed as a function of superficial gas velocity is shown in Figure 2.2.

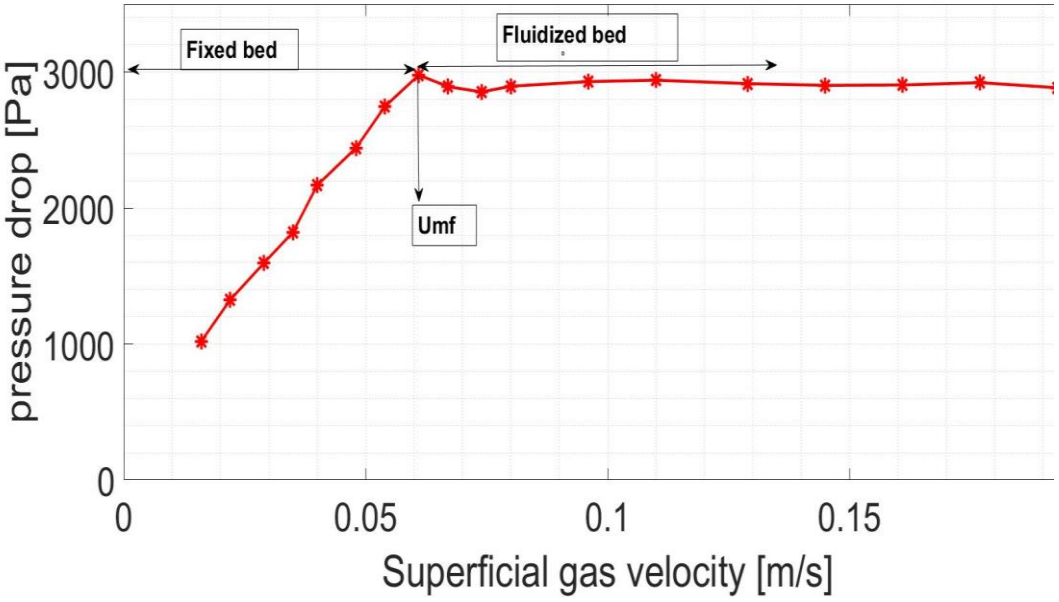

Figure 2.2:pressure drop vs superficial gas velocities profile of sand particles with mean diameter (234.7µm)

During the onset of fluidization:

$$\begin{Bmatrix} pressure\ drop \\ across\ bed \end{Bmatrix} \begin{Bmatrix} cross\ sectional \\ area\ of\ tube \end{Bmatrix} = \begin{Bmatrix} volume \\ of\ bed \end{Bmatrix} \begin{Bmatrix} fraction \\ consisting \\ of\ solids \end{Bmatrix} \begin{Bmatrix} specific \\ weight \\ of\ solids \end{Bmatrix}$$

or

$$\Delta p_b A_t = A_t L_{mf}(1-\varepsilon_{mf})\left[\left(\rho_s-\rho_g\right)\frac{g}{g_c}\right] \quad 2.1$$

$$\frac{\Delta p_b}{L_{mf}} = (1-\varepsilon_{mf})\left[\left(\rho_s-\rho_g\right)\frac{g}{g_c}\right] \quad 2.2$$

Where , $g_c\left[\frac{9.8kg.m}{kg-w.s^2}\right]$ is a conversion factor

The frictional pressure drop across the bed for isotropic solids is given by Ergun[12] as:

$$\frac{\Delta p_{fr}}{L_m} g_c = 150\frac{(1-\varepsilon_m)^2}{\varepsilon_m^3}\frac{\mu\mu_0}{(\phi_s d_p)^2} + 1.75\frac{1-\varepsilon_m}{\varepsilon_m^3}\frac{\rho_g \mu_0^2}{\phi_s d_p} \quad 2.3$$

Solving equations 3.2 and 3.3 gives:

$$\frac{1.75}{\varepsilon_{mf}^3\phi_s}\left(\frac{d_p u_{mf}\rho_g}{\mu}\right)^2 + \frac{150\left(1-\varepsilon_{mf}\right)}{\varepsilon_{mf}^3\phi_s^2}\left(\frac{d_p u_{mf}\rho_g}{\mu}\right) = \frac{d_p^3\rho_g(\rho_s-\rho_g)g}{\mu^2} \quad 2.4$$

$$\frac{1.75}{\varepsilon_{mf}^3\phi_s}\mathrm{Re}_{p,mf}^2 + \frac{150\left(1-\varepsilon_{mf}\right)}{\varepsilon_{mf}^3\phi_s^2}\mathrm{Re}_{p,mf} = Ar \quad 2.5$$

Where, the Archimedes number(Ar) is defined as:

$$Ar = \frac{d_p^3\rho_g(\rho_s-\rho_g)g}{\mu^2} \quad 2.6$$

Since u_{mf} is an essential design parameter that largely influences the fluidization properties, it is vital to calculate its value appropriately. Several models have been proposed for the theoretical calculations of u_{mf} and these models vary for different particles and process conditions, thus, the models must be verified with the experimental analysis.

Anantharaman et al. made a broad comparison of u_{mf} value and its discrepancies predicted by the different correlations applied to Geldart Groups A, B and D particles. They highlighted the reasons for disparity in u_{mf} prediction by different models as: empirical data fitting based on limited experiments, use of empirical coefficient as an exponent, insufficient knowledge of cohesive forces associated with Geldart Group A particles [13].

Felipe et al. evaluated the minimum fluidization velocities in gas-solid fluidized bed by the pressure fluctuation measurements (standard deviation methodology) for four particles, Sand, Microcrystalline Cellulose, Alumina and FCC. They validated the methods comparing the u_{mf} results obtained from a fluid-dynamic curve[5].

Jena et al. measured the fluidization velocity of homogenous well mixed ternary mixtures of three different particle size with different composition in square beds (un-prompted and rod-prompted). They found that the minimum fluidization velocity and bed voidage decrease with increase in the mass fraction of fines in the mixtures. Also, the theoretical values of the minimum fluidization velocities calculated using Wen and Yu were close to the experimental values obtained[14].

David et al. studied the effects of bed height and material density on minimum fluidization velocity and gas holdup using 3D cylindrical fluidized bed of diameter 10.2 cm. They used three different Geldart type-B particles, ground walnut shell, glass beads & ground corncob, with particle size distribution of 500-600 µm and densities 1300, 2600, 1000 kg/m^3 respectively. Three different aspect ratios, H/D=0.5, 1, 1.5, 2, 3, were used to investigate minimum fluidization velocity and local time-average gas holdup values. Based on the results obtained, they suggested that minimum fluidization velocity and bed hydrodynamics were independent of bed height while, it varied with change in densities of particles[4].

Sarker et al. used two laboratory scale fluidized bed (diameter: 12.5 cm and 3.5 cm) to investigate the effect of bed diameter, bed height and particle shape on pressure drop and minimum fluidization velocity. They varied the bed height form 2 cm to 7 cm and particle size of 0.85 mm to 1 mm were chosen. They observed incipient minimum fluidization, bubble shape, bubble flow and particle collisions in the fluidization regimes using digital imaging. From the experiments data, they concluded that minimum fluidization velocity does not show significant variation due to change in bed height while, it decreases with decrease in bed diameter. Also, they observed that the pressure drop required to reach minimum fluidization for the bed with non-spherical particles is lower compared to spherical particles[3].

Table 2.1:Minimum fluidization velocity correlations

Author	$d_p(\mu m)$	$\rho_p(kg/m^3)$	u_{mf} (Correlation)
Bourgeois et al.[15]	86-25000	1200-19300 (A, B, D)	$\mathrm{Re}_{mf} = (25.46^2 + 0.0382Ar)^{0.5} - 25.46$
Babu et al.[16]	50-2870	2560-3920 (A, B, D)	$\mathrm{Re}_{mf} = (25.25^2 + 0.0651Ar)^{0.5} - 25.25$
Wen-Yu	2052-6350	2360-7840 D	$\mathrm{Re}_{mf} = (33.7^2 + 0.048Ar)^{0.5} - 33.7$

2.2 Bubbling Regime

The average fluidization velocity at which the bubbles first start to appear and disappear in the bed is called the minimum bubbling velocity. The growth of bubble in the bed largely depends on particle properties (density, size, distribution) and gas properties. It has been observed that for the bed with larger particles (Geldart particle type B) the bubble formation starts as soon as the superficial gas velocity pasts the minimum fluidization velocity. However, for smaller size bed particles, for instant, FCC, the bed expands significantly with the increase in superficial gas velocity beyond fluidization velocity and further increases in gas velocity initiate the bubbles formation in the bed. Minimum Bubbling velocity for smaller particles in the bed is proposed by Geldart and Abrahamsen [6]:

$$U_{mb} = 2.07 \exp(0.716F) \frac{d_p \rho_g^{0.06}}{\mu^{0.347}} \qquad 2.7$$

Where, F is the mass fraction of the powder less than 45μm.

Fluidizing index is the ratio of minimum bubbling velocity to minimum fluidization velocity, that determines the extent up to which bed can expand uniformly[1]

$$\frac{\mu_{mb}}{\mu_{mf}} = \frac{2300 \rho_g^{0.13} \mu^{0.52} \exp(0.72 P_{45\mu m})}{\bar{d}_p^{0.8} (\rho_s - \rho_g)^{0.93}} \qquad 2.8$$

2.2.1 Bubble size and bubble rise velocity

The bubble shape, size and bubble rise velocity are among some of the major dynamic characteristics of fluidized bed that plays key roles in a design of gas-solid fluidized bed reactors. Several models have been established to calculate the bubble shape and bubble rise velocity in fluidized bed. The gas velocity further increased after minimum fluidization contributes to form bubble termed as bubble gas. The bubble gas velocity can be expressed as:

$$u_b = \psi A_t (u_0 - u_{mf}) \qquad 2.9$$

Where, ψ ratio of observed bubble flow to that expected from two phase theory,

A_t, Cross section area of the bed

u_b, Velocity of bubble rising through a bed and u_0 is superficial gas velocity

Hilligardt and Werther[17] proposed ψ for $z/d_t \cong 1$, as 0.8, 0.65 and 0.26 for Geldart A, B and D particles. Further Werther[8] proposed bubble rise velocity that accounts for all range of Geldart particle types and vessel size

$$u_b = \psi A_t (u_0 - u_{mf}) + a u_{br} \qquad 2.10$$

Where,

Geldart-type particle	A	B	D
a	$3.2 d_t^{\frac{1}{3}}$	$2.0 d_t^{\frac{1}{2}}$	0.87
$d_t(m)$	0.05-1.0	0.1-1.0	0.1-1.0

u_{br} can be calculated from Davidson and Harrison[18] model for bubble rise velocities:

For single bubbles:

$$u_{br} = 0.711 (g d_b)^{0.5} \qquad 2.11$$

Similarly, the expression for bubble size at any height z in a bed of Geldart particle B is proposed by Werther [8] as:

$$d_b(cm) = 0.853\left[1 + 0.272\left(u_0 - u_{mf}\right)\right]^{1/3} \left(1 + 0.0684 z\right)^{1.21} \qquad 2.12$$

Conditions:

$d_t > 20cm$ $\qquad$ $1 \le u_{mf} \le 8cm/s$

$100 \le d_p < 350\mu m$ $\qquad$ $5 \le u_0 - u_{mf} \le 30cm/s$

2.2.2 Bubble behavior in different Geldart Particle types

Bubble behavior in fluidized bed depends on the mean particle properties (mean particle size and density) and gas properties. Geldart recognized the characteristic behavior of particles at ambient air condition and categorized in a group of four, namely Geldart group A, B, C and D, shown in Figure 2.3.

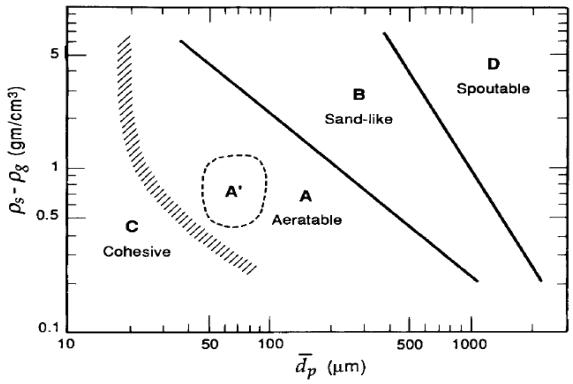

Figure 2.3: Geldart classification of particles for air at ambient conditions[1]

Group C

Very fine and cohesive particles like flour, face powder, and Starch lies in this group. These particles don't show bubbling behavior.

Group A

Aerated particles small is size (< 45μm) and density (< ~ 1.4 g/cm^3) for example: FCC catalyst lies under this category. These particles can easily fluidize, and rapid bubbles appear at the velocities higher than U_{mb} which can be calculated using equation 2.7.

Group B

The particles with mean diameter $40\mu m < \bar{d}_p < 500\mu m$ and density $1.4 < \rho_s < 4g/cm^3$ lies in the Geldard group B. The particles fluidized as soon as it reaches minimum fluidization i.e. $u_{mf}/u_{mf} \cong 1$. With this particle in fluidized bed, small bubbles form at the lower level of bed and grow linearly above the distributor and coalesce as they rise at the top. Since vigorous bubbling contributes to the gross circulation of solids inside the bed, most of the gas-solid reactions like metallurgical reactions are performed in this regime.

Group D

Dense and spoutable particles that are difficult to fluidized lies in this category. During the fluidization the bubbles grow more rapidly resulting in sever channeling or spouting behavior of the bed. However, in the processes like chemical agglomeration and processing of agricultural products this behavior of bed is unavoidable.

2.3 Slugging Regime

With the increase in superficial gas velocities, the bubble diameter, D_e, increases. When the bubble diameter is ~0.3- 0.6 D, the bed slugs and the type of slugs appeared in the bed depends on particle type, size, bed diameter and the wall of the column. Basically, axisymmetric slugs occur in the bed with Geldart A particles while, Square -nosed slugs are likely to occur in bed with Geldart D particles when the bed diameter, D, is small. In this case, the particles rain through the slugs (Figure 2.4 (c)). When the walls of the fluidized bed are rough, slugs appear around the wall surface as shown in Figure 2.4 (b). Rudolph and Judd[19] proposed rise velocity of square nosed slugs as:

$$U_{S\infty} = 0.18\sqrt{gD} \qquad 2.13$$

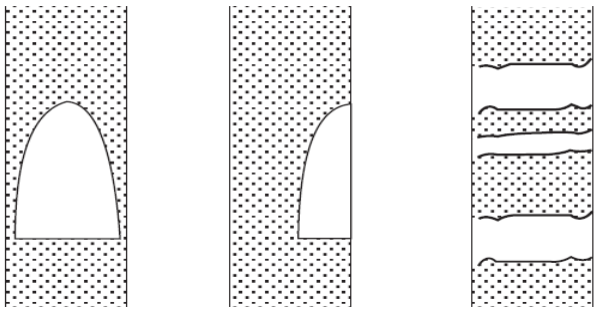

(a) (b) (c)

Figure 2.4: Types of slug: (a) axisymmetric, (b) wall and (C) square-nosed slugs

Similarly, the rise velocity of a single axisymmetric slug in a fluidized bed is proposed by Stewart and Davidson[20] as:

$$U_S = 0.35\sqrt{gD} \qquad 2.14$$

With excess gas velocity, $U - U_{mf}$, for continuously formed axisymmetric slugs the rise velocity of a single slug (using two-phase theory) in freely-slugging bed can be given as[7]:

$$U_S = U - U_{mf} + 0.35\sqrt{gD} \qquad 2.15$$

Similarly, a slug in a bed with a small diameter can occur if the superficial gas velocity is sufficient enough to excess the minimum slug velocity and minimum slugging velocity proposed by Stewart and Davidson as[20]:

$$U_{ms} = U_{mf} + 0.07\sqrt{gD} \qquad 2.16$$

However, Baeyens and Geldart [21] proposed that Equation 2.16 is only valid if $H_{mf} > 1.3D^{0.175}$ (where, H_{mf} and D are in meters) and they suggested U_{ms} as:

$$U_{ms} = U_{mf} + 0.07\sqrt{gD} + 0.16(1.3D^{0.175} - H_{mf})^2 \qquad 2.17$$

Slug formation and rise velocities are important dynamic characteristics of gas-solid fluidized bed that affect the contact area of fluidizing gas and solids thus, influence the overall chemical conversion. In case of commercial scale fluidized bed reactor slugging is unlikely to occur. The regime shifts from bubbling to turbulent.

In this work two correlation for minimum slugging velocity proposed by Baeyens and Geldart and Agu et al.[22] is used to compare the experimental and simulation results. According to Agu et al. the slugging velocity in deep fluidized bed can be obtained as:

$$\frac{U_{bs}}{U_{mf}} = 1 + 2.33U_{mf}^{-0.027}(\varphi^{0.35}c_t^{a_t} - 1)\left(\frac{h_0}{D}\right)^{-0.588} \qquad 2.18$$

Where, $c_t = c_b / c_s$ and $a_t = 1/(a_s - a_b)$

Table 2.2: Correlations for the proposed model parameters a and c

Parameters	Expression	Validity
a	$0.725 + 0.230\log(Ar)$	$\log(Ar) < 3.9$
	$1.184 + 8.962\times10^{-1.35}$	$\log(Ar) \geq 3.9$
c	$0.042 + 0.108\log(Ar)$	$\log(Ar) < 4.0$
	$(0.978 - 1.964\times10^{2}\,Ar^{-0.8})^{4.88}$	$\log(Ar) \geq 4.0$

2.4 Turbulent Regime

For the fluidized bed with small particles, increase in superficial gas velocity beyond bubbling velocity, there is random fluctuation of pressure drop across the bed and these fluctuation reach a peak value at u_c, decline and reach a steady value u_k with the increase in superficial gas velocity as shown in Figure 2.5. Random fluctuation of the pressure drop is due to rapid breakup and coalescence of the bubbles in the bed. The onset of transition from slug to turbulent regime is marked at a peak value (corresponding to the highest pressure drop at superficial gas velocity u_c) .[10].

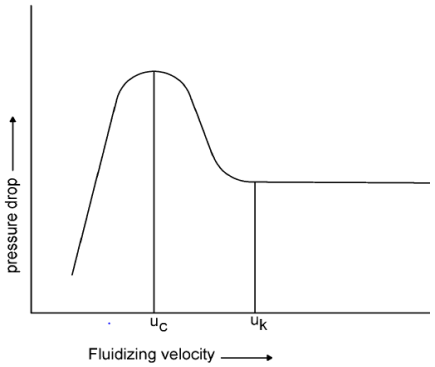

Figure 2.5:Amplitude of pressure Fluctuation with increase in gas velocity

Grace et al. proposed some correlations for u_c and u_k based on small bed diameter as:

$$u_c = 3\sqrt{\rho_p d_p} - 0.17 \qquad 2.19$$

$$u_k = 7\sqrt{\rho_p d_p} - 0.77 \qquad 2.20$$

Horio et al. proposed an alternative set of equations for the transition from u_c to u_k as[23]:

$$\mathrm{Re}_c = \frac{u_c d_p \rho_g}{\mu} = 0.936 Ar^{0.472} \qquad 2.21$$

$$\begin{aligned} \mathrm{Re}_k &= \frac{u_k d_p \rho_g}{\mu} = 1.46 Ar^{0.472} \quad (Ar < 10^4) \\ \mathrm{Re}_k &= \frac{u_k d_p \rho_g}{\mu} = 1.46 Ar^{0.56} \quad (Ar > 10^4) \end{aligned} \qquad 2.22$$

Similarly, Bi and Grace et al.[24] proposed model form minimum turbulent velocity as:

$$u_c = (0.56 \times Ar^{0.464} \times \mu_g) / (\rho_g \times \rho_p) \qquad 2.23$$

The turbulent regimes are marked with the absence of bubbles and slugs in the bed and followed by violent movement of elongated and distorted voids of particles. The particles at the top of the bed are continuously ejected into freeboard. Unlike coarse particles, fine particles in fluidized bed enters turbulent fluidization at a velocity above the terminal velocity. In case of coarse particles, for instant Geldart D particles, large exploding bubbles are absorbed before the turbulent regime is reachds. Once the turbulent regime is stablished, it is followed by severe channeling and large-scale gross circulation of bed material uniformly termed as “churning fluidization”[1].

3 Methods to Identify Fluidization Regimes

For the efficient applications for instance uniform heat transfer and solid circulation, optimal design of fluidized bed reactors is essential. Identification of different fluidized bed regimes: minimum fluidization, bubbling, slugging and turbulent regimes are essential since different process are carried out at specific regime. The fluidized bed regimes can be established using methods: Visual observation, analyzing average physical properties (solid volume fraction, pressure fluctuation) with respect to time. Commonly used methods such as standard deviation of pressure fluctuation and solid void-fraction analysis are discussed in this chapter. Identifying the onset and transition of one regime to another using the fluctuation of pressure drop and void fraction across the bed are most widely used methods. In this study the standard deviation of pressure fluctuations across different sections of bed were used to identify the regimes and its transition zone.

3.1 Standard Deviation

Standard deviation is a statistical analyses technique that uses statistical parameters (example: pressure and void fraction) as a function of superficial gas velocity to identify different regimes in a gas-solid fluidized bed. Standard deviation is evaluated by the square root of its variance as in equation 2.1. Basically, standard deviation shows the measure of the variation of (N) data sets from its mean value ($\overline{p}$).

$$\sigma = \sqrt{\frac{\sum_{i=1}^{N}\left(P_i - \overline{P}\right)^2}{N-1}} \qquad 3.1$$

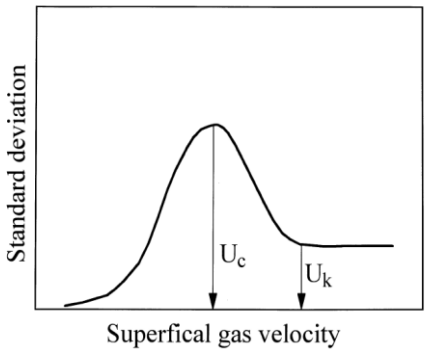

Figure 3.1: Schematic diagram of standard deviation curve

The change in standard deviation (of pressure fluctuation) can be used to identify the onset or transition of one regime to another as shown in Figure 3.1. The onset of one regime to another is marked by the point where there is change in a slope of the standard deviation cure. This method has been widely used by the researches to identify the minimum fluidization velocity and quality of fluidization [5, 25-27]. Similarly, Different regimes in fluidized bed have been identified using standard deviation and compared with other techniques [28, 29].Yerushalmi and Cankurt [10] identified turbulent flow regimes with two transition velocities as shown in Figure 3.1. Further, Bi et al.[24] identified transition of turbulent regime using the same method and proposed that the value of u_c is higher for the differential pressure than absolute pressure.

4 Experimental setup and procedure

4.1 Equipment

The experimental set up used in this work consists of a 3D transparent cold bed column of height 1.5 m and diameter 0.084 m. A set of pressure transducers are connected to the pressure tapping points installed along the wall of the column. The distance between two consecutive pressure points along the column height is 10 cm. Compressed air at an ambient condition was supplied through an air supply hose fitted at the bottom of the column. Air flow from the compressor into the column was controlled by the control valve attached to the rig. Figure 4.1 (a) schematic diagram of the position of the pressure tapping points and the air distributor along the column and (b) Experimental rig.

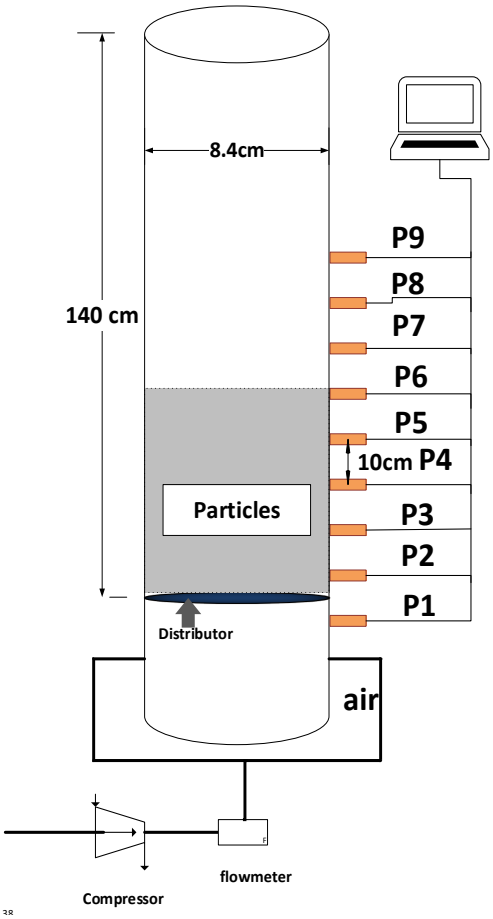

(a)

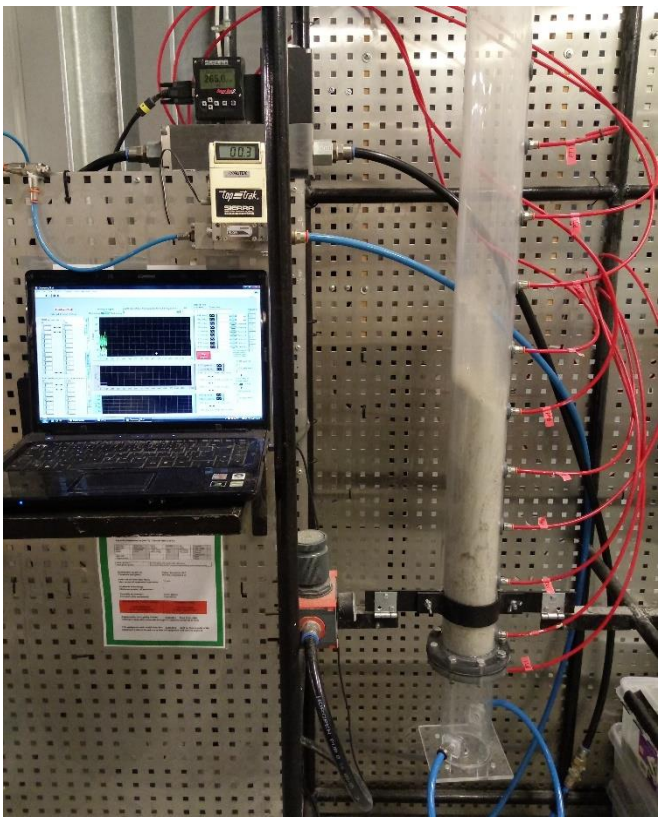

(b)

Figure 4.1:(a) Schematic diagram of experimental setup (b) Experimental rig

4.2 Procedure

The particles were added in the column from the top before the experiment started and superficial air velocity (compressed air at ambient condition) was increased gradually (controlled using control valve) and pressure drop due to increase in velocity was logged in LabVIEW via pressure sensors attached along the cold bed column. For each flow, data were logged for more than 1 minute (with sampling time of 1s) and minimum of 60s were allowed to establish the flow before the data were logged. The particles were removed from the column after each experimental series since, the fluidized bed particles exhibit different properties once it is fluidized**.** The pressure drop at each tapping points for each flow rate was calculated by subtracting the distributor pressure at corresponding flow rate as shown in equation 4.1. The data acquired in the LabVIEW were imported to MATLAB (see Appendix B for the code).

$$\Delta P_{1,f_i} = P_{1,f_i} - DP_{f_i} \qquad 4.1$$

Where, P_1 pressure at pressure tapping point 1

DP distributor pressure

f_i air flowrate

4.3 Particles selection and Sieve analysis

In this work three different particles, sand (2 sizes), limestone and glass beads, were used and their properties like mean diameter and particle size distribution were identified using sieving analysis. The particles with different properties and size distribution were selected to analyse their influence on the hydrodynamic behavior of the fluidized bed regimes. The selection of particles is based on the criteria: fluidization behavior, size range and density. Sand and limestone particles with different size distributions were used to investigate the influence of size distribution on the bed regimes and the transition zones. Similarly, glass bead are uniform, spherical and non-adhesive particles that may exhibit better fluidization quality. Unlike glass beads, limestone and sand particles are irregular and adhesive, which affect the fluidization quality adversely. The particle mean diameter were calculated using equation 4.2. Properties of bed materials used in this work are presented in Table 4.1-4.4.

$$d_m = \frac{1}{\sum\left(\frac{w_s}{d_s}\right)_i} \qquad 4.2$$

Table 4.1:Bed Properties-Sand particle

Particle mean diameter		234.74 µm		
Density		2650kg/m^3		
Bulk density		1388.17 kg/m^3		
Solid void fraction		0.52		
Particle size distribution				
Sieve range (µm)	Radius (m)	Particle weight (g)	Weight fraction	Cumulative (%)
100-150	0.0000625	1.37	0.028376139	2.837614
150-200	0.0000875	5.59	0.115782933	14.41591
200-250	0.0001125	15.48	0.32062966	46.47887
250-300	0.0001375	25.84	0.535211268	100

Table 4.2:Bed Properties-Sand particle

Particle mean diameter		346.35 µm		
Density		2650 kg/m^3		
Bulk density		1391.45 kg/m^3		
Solid void fraction		0.52		
Particle size distribution				
Sieve range (µm)	Radius (m)	Particle weight (g)	Weight fraction	Cumulative (%)
200-250	0.0001125	1.37	0.02076061	2.076061
250-300	0.0001375	5.59	0.073672607	9.443322
300-355	0.0001638	15.48	0.419070366	51.35036
355-425	0.000195	25.84	0.486496417	100

Table 4.3:Bed properties-Limestone

Particle mean diameter		672 µm		
Density		2837 kg/m^3		
Bulk density		1348.3 kg/m^3		
Solid void fraction		0.47		
Particle size distribution				
Sieve range (µm)	Radius (m)	Particle weight (g)	Weight fraction	Cumulative (%)
450-500	0.000238	1.98	0.037302185	3.721805
500-600	0.000275	10.42	0.19630746	23.30827
600-710	0.000328	18.95	0.357008289	58.92857
710-850	0.00039	17.31	0.32611153	91.46617
850-1000	0.000463	4.42	0.083270535	99.77444
1000-1400	0.0006	0.12	0.002260739	100

Table 4.4:Bed Properties-Glass beads

Particle mean diameter		329.5 µm		
Density		2500 kg/m^3		
Bulk density		1722.39 kg/m^3		
Solid void fraction		0.68		
Particle size distribution				
Sieve range (µm)	Radius (m)	Particle weight (g)	Weight fraction	Cumulative (%)
200-300	0.000125	20.3	0.364845435	36.48454
300-425	0.000181	2.5	0.044931704	40.97771
425-500	0.000231	8.57	0.154025881	56.3803
500-600	0.000275	5.28	0.094895758	65.86988
600-710	0.000328	3.32	0.059669303	71.83681
710-850	0.00039	15.67	0.281631919	100

5 Simulation set-up and procedures

While dealing with particle fluid flow, problems such as complex geometries, extreme operational conditions, comprehensive study of the bed interior etc. are likely to be encountered. Unlike experiments, simulation can easily handle these difficulties economically and within specific time. In this work, it was difficult to establish the turbulent regime due to limited height of the cold bed column. Thus, modelling using the Computational Particle Fluid Dynamic (CPFD) software Barracuda V.R, was used to establish the hydrodynamic flow regimes. This chapter discusses the simulation set up used in the Barracuda for the simulations. Similarly, the procedures to validate the CPFD model with experimental result are discussed in section 5.2.

5.1 Simulation Set up

A cylindrical CAD geometry similar to the column used in the experiment, height 300 cm and diameter 8.4 cm, was imported in Barracuda VR. Uniform grid of total 10000 cells were established around the geometry for the simulations. The bottom of the column was set up as inlet flow boundary condition while the top of the column was considered as the pressure boundary condition (as in the experimental set up). Thus, gas flow was throughout the column with no boundary layer around the walls. The cells with volume fraction less than 0.04 and aspect ratio greater than 15:1 were removed since, default grids were generated using default settings. The monitoring points were selected at the middle of the column and height equivalent to the pressure transducers location in the experiment. The CAD geometry, grid, flow and pressure boundary conditions and transient data locations used in the simulations are shown in Figure 5.1.

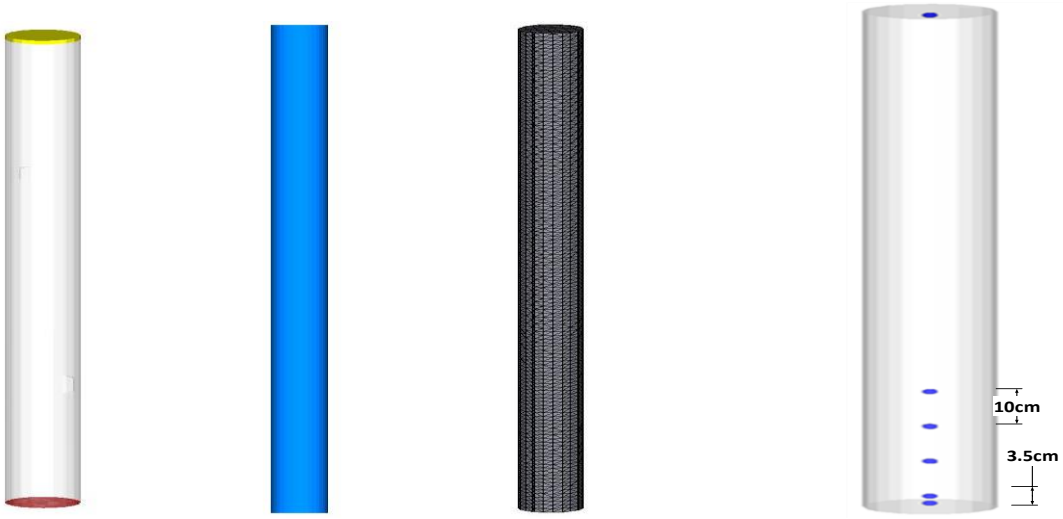

(a) (b) (c) (d)

Figure 5.1:(a) flow and pressure boundary conditions, (b) CAD geometry, (c) Grid (d) pressure reading points

The particles like sand (SiO_2), Limestone and glass were used as the base materials and air at ambient conditions as the fluidizing gas. The particle size distribution and close pack volume fraction used for the simulations were same as in the experiment. The maximum momentum from redirection of particles collision were assumed to be 40% with normal-to-wall and tangential-to-wall momentum retention as 0.3 and 0.99 respectively. The particle properties and operating conditions used in the simulations are summarized in Table 5.1.

Table 5.1: Operating conditions

Fluidizing Gas	Air
Fluid temperature	Ambient (300K)
Superficial gas velocity	0.016 to 2.5 m/s
Static bed heights	(0.7, 1, 1.5, 2, 2.5) D
Outlet pressure	101325 Pa

5.2 Procedures

5.2.1 Model validation

To establish a valid model for further simulations, the simulations and experiments were done with the sand particles (Figure 5.2) and aspect ratio (H/D) 2.5 and the results regarding minimum fluidization velocity obtained by plotting pressure drop versus superficial gas velocity were compared as shown in Figure 5.2. The figure shows the minimum fluidization velocity of sand particles from simulations using Wen-Yu & Ergun model and Wen-Yu model. The results from Wen- Yu Ergun drag model predicts close to the experimental values while Wen- Yu model over predicts the minimum fluidization. Thus, Wen-Yu & Ergun drag model is use in rest of the work. The deviation in Wen-Yu and Ergun drag model is about 9%, which could be due to difference in particle size distribution and solid volume fraction compared to experiments.

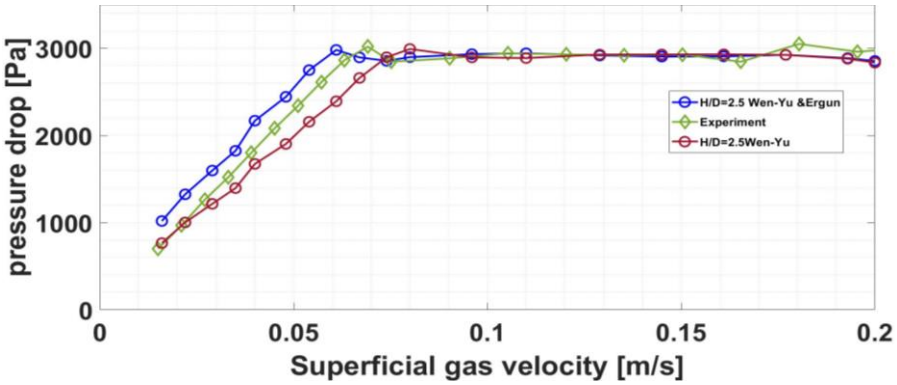

Figure 5.2: Pressure drop vs superficial gas velocity using two drag models and experimental results for a model validation

6 Experimental and simulation results

In this section, the results from the experiments for four different particles, mentioned in the Table 4.1-Table 4.4, are presented. The minimum fluidization velocity for each type of particles and aspect ratios are discussed in Chapter 6.1 and different regimes, as a function of superficial gas velocity and pressure fluctuation, are identified in Chapter 6.2. Due to limited height of the column, increase in superficial gas velocities to establish turbulent regime experimentally was not possible. Thus, the turbulent regime has been identified based on the simulation results. The simulation results used in this chapter are from the validated CPFD model established in Chapter 5.

6.1 Minimum fluidization velocity

The minimum fluidization velocity for each aspect ratios and four different particles (sand, limestone, glass beads) were identified by plotting pressure drop versus superficial gas velocity obtained from the experimental data.. Figure 6.1 and Figure 6.2. shows the change in pressure drop with respect to change in superficial gas velocity for sand particles ($d_m = 346.3\mu m$), and limestone ($d_m = 672\mu m$) respectively. The minimum fluidization velocity was identified at the point of maximum pressure drop and the minimum fluidization velocity for limestone and sand particle ($d_m = 346.3\mu m$) were found to be $0.12\ m/s$ and $0.36 m/s$ respectively. Also, it was discovered that the minimum fluidization velocity remained almost unchanged with increase in aspect ratio for two particles limestone and sand.

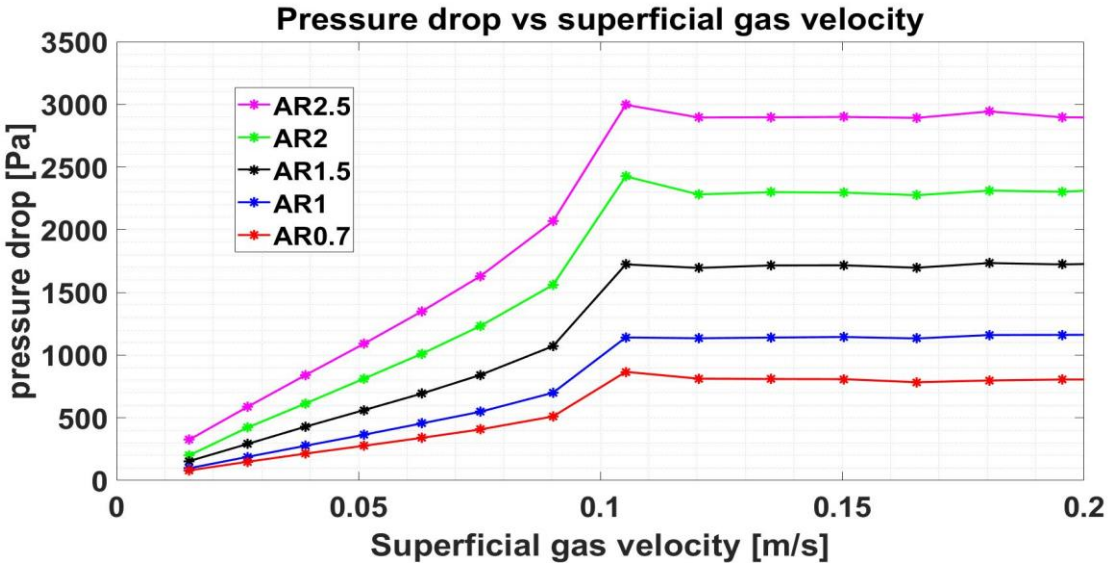

Figure 6.1: Minimum fluidization velocity for sand particle (200-400µm)

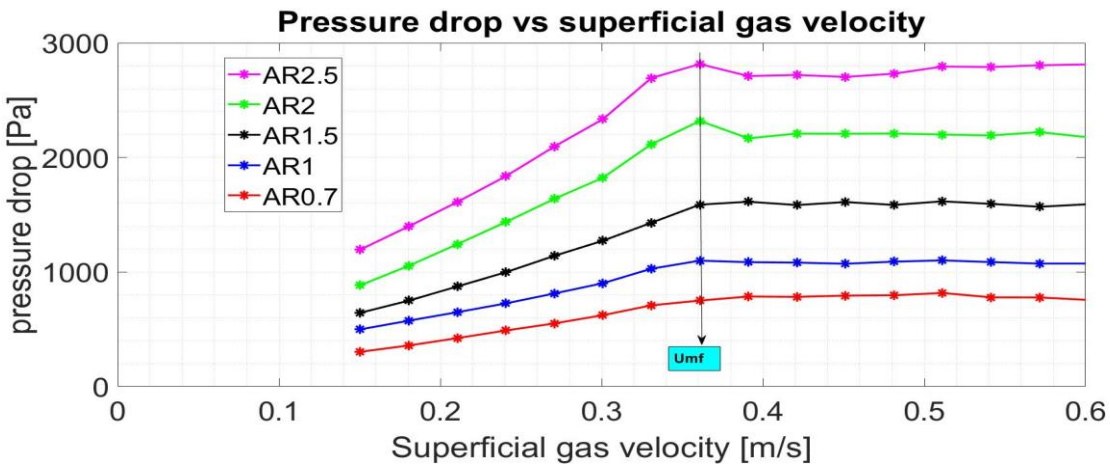

Figure 6.2:Minimum fluidization velocity of limestone (400-1400µm)

Figure 6.3 shows the minimum fluidization velocity for sand particles ($d_m = 234.7\mu m$) obtained from the experimental data. The minimum fluidization was identified at the point of maximum pressure drop obtained by plotting pressure drop versus superficial gas velocity. Unlike limestone, the minimum fluidization velocity increases with increase in as aspect ratio > 1.5 from $0.5\ m/s$ to $0.6\ m/s$. Similarly, the minimum fluidization velocity for glass beads decreases with decrease in aspect ratio < 2.5 form $0.065\ m/s$ to $0.035\ m/s$ as shown in Figure 6.4

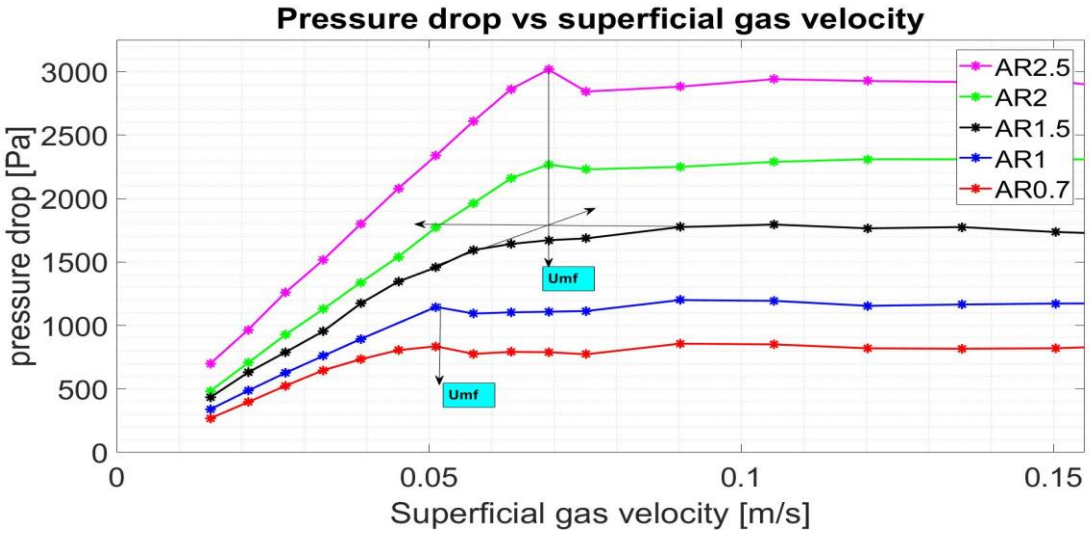

Figure 6.3:Minimum fluidization velocity of sand particles (100-300µm)

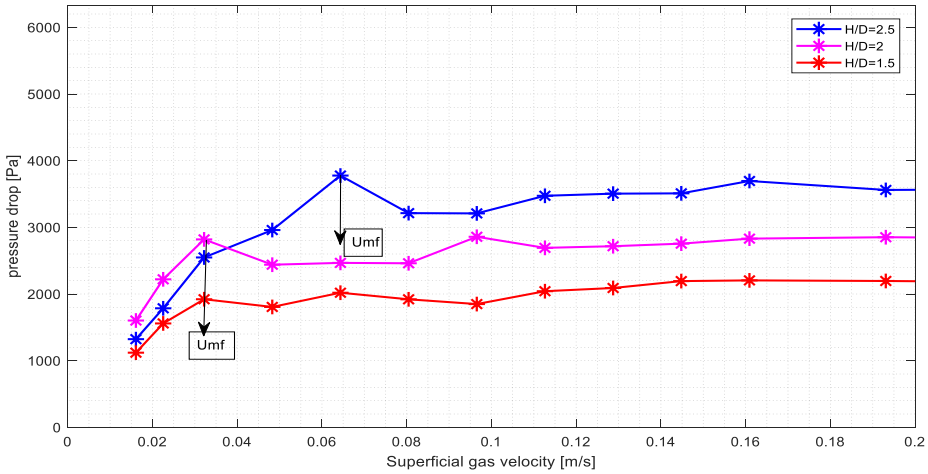

Figure 6.4: Minimum fluidization velocity of glass beads

6.2 Regimes identification using statistical method

Different flow regimes namely: Bubbling, slugging and turbulent regimes, for each aspect ratio were identified via standard deviation of pressure fluctuation as a function of superficial gas velocity. The pressure measuring points were selected inside the bed and onset of a regime or transition of one regime to another is marked at the point of change of slope in the curve. Tofurther confirming the results obtained from pressure fluctuation (standard deviation), the results were analyzed by measuring the fluctuation of solid volume fraction inside the bed for each time step and flowrate. The flow regimes are identified using the simulation results obtained from the validated CPFD model.

Figure 6.5 shows the standard deviation of pressure fluctuation as a function of superficial gas velocity, simulated for the sand particle ($d_m = 346.3\mu m$) and aspect ratio of 0.7. The standard deviation curve shows that the pressure fluctuation remains constant until, it reaches superficial gas velocity corresponding to minimum bubbling velocity, U_{mb}, marked as the onset of bubbling regime. The pressure fluctuation increases sharply beyond this gas velocity. The fluctuation of pressure drop at this stage is due to formation and coalescence of the bubbles inside the bed. With the further increase in superficial gas velocity, the bubbles size increases large enough and the bed transits to the slug regime. The superficial gas velocity at which the bed slug, is denoted as U_{ms} as shown in Figure 6.5. The rate of change of pressure fluctuation decreases at this stage. As the superficial gas velocity increases to critical velocity, U_C, the slug explodes resulting in vigorous movement of bed, marked as the onset of turbulent regimes. In this regime, the particles were observed to remain separated and in motion with the absence of bubbles and slugs in the bed. Further increase in gas velocity, the pressure fluctuation reaches steady value as shown in Figure 6.5.

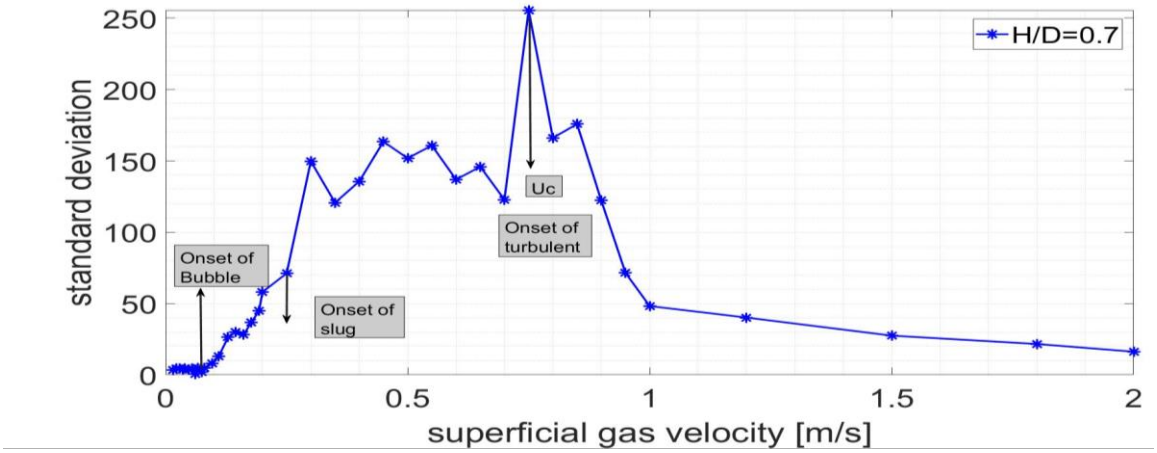

Figure 6.5: Pressure drop fluctuation showing onset of different regimes

For each of the regimes identified in Figure 6.5, the fluctuation of solids fraction in the bed is shown in Figure 6.6. Within the time interval 80 - 90 s for gas velocity 0.064 m/s, it can be seen that the particle solid volume fraction decreased from 0.52 to a value of about 0.5, marking the point of minimum fluidization condition. The solid fraction remained constant up to 100 s and started to drop from 0.5 to 0.35 in the period of 100 - 110 s and flowrate 0.07, marking the onset of bubbling regime. Similarly, the onset of slugging regime is identified at the flowrate of 0.25 m/s and time period 190 - 200 s. The onset of turbulent regime can be confirmed at the flow rate of 0.75 m/s and at time 290 - 300 s. At this gas velocity, the fluctuation in solids fraction is vigorous, corresponding to the peak value of the pressure fluctuation in Figure 6.5.

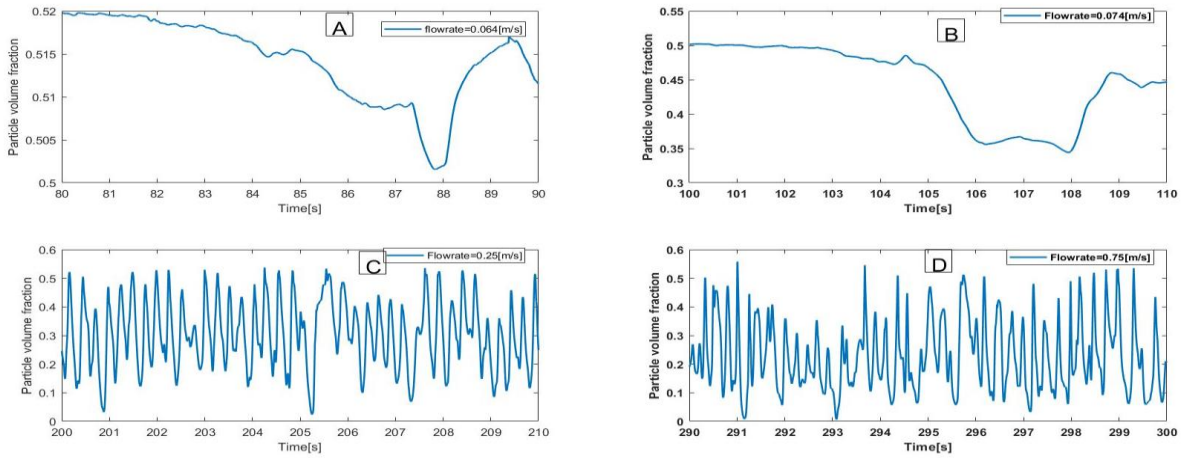

Figure 6.6: Change in solid volume fraction at the onset of different fluidization regime (A)minimum fluidization (B) minimum bubbling regime (C) minimum slugging regime (D) minimum turbulent regime

7 Analysis and Discussion

In this chapter, the influence of bed height, particle density and particle size distribution on different fluidized bed regimes are discussed. Similarly, the experimental and simulation results for different regimes are compared with the established mathematical correlations.

7.1 Influence of bed height, particle density and size distribution on fluidized bed regimes

7.1.1 Minimum Fluidization

Figure 7.1 shows the minimum fluidization behavior of sand and limestone particles with varying aspect ratios, density and mean diameter. It can be seen from the figure that the minimum fluidization velocity increases with increase in density of the particles i.e. the U_{mf} , $0.38\ m/s$, for limestone is found to be higher than the sand particles. Further, when the particle mean diameter is increased, keeping the density constant, it is found that the U_{mf} value is increased. This is noticeable with the sand particles. For the sand particle with mean diameter 346µm, the U_{mf} is found to be $0.14\ m/s$. While, for sand particle with same density but mean diameter of 234µm, the U_{mf} is about $0.068\ m/s$.

The minimum fluidization velocity seems to be independent of static bed height for two particles limestone and sand. However, for sand ($d_m = 234\mu m$), the minimum fluidization velocity tends to decrease when $\frac{H}{D} > 1.5$. This is due to the presence of small size particles in the bed which enables the bed to fluidize at lower superficial gas velocities when the static bed height is lowered. This trend was found opposite in case of simulation, this could be due to absence of distributor in case of simulation unlike experiment.

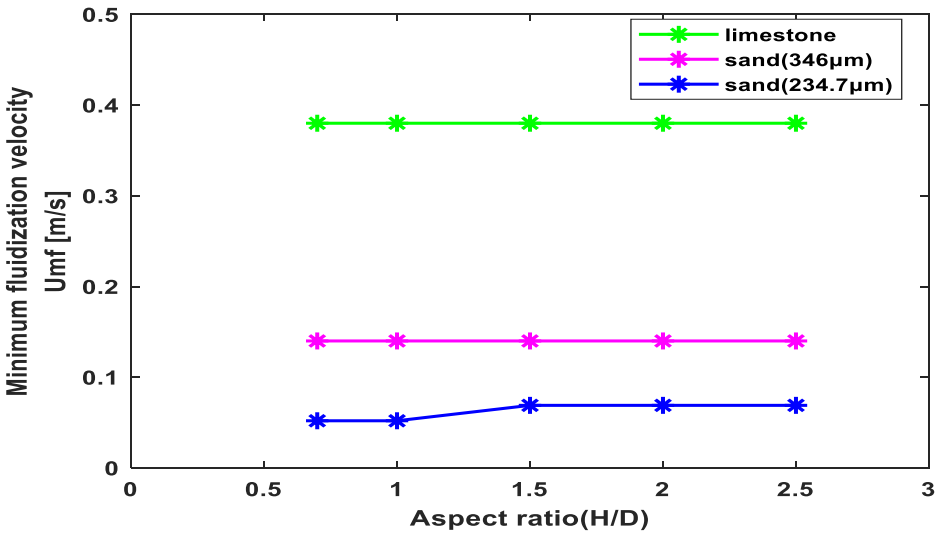

Figure 7.1: Change in minimum fluidization velocity with change in aspect ratio

7.1.2 Minimum bubbling velocity

The onset of bubbling regime for three different particles and different aspect ratios show similar behavior as that of minimum fluidization velocity i.e. minimum bubbling velocity is found to be independent of the aspect ratio for all three types of particles. This is because all three types of particles are Geldart particles type B, which start to bubble as soon as is the bed is fluidized. The relation between minimum bubbling velocity and change in the aspect ratio is shown in Figure 7.2. Like minimum fluidization velocity, U_{mb} increase with increase in particle size and particle density. For limestone ($d_m = 672\mu m$) minimum bubbling velocity is found to be 0.46 m/s, while for sand ($d_m = 234\mu m$), U_{mb} is 0.74 m/s. For the sand particle when the mean diameter is increased the minimum bubbling velocity increases to 0.18 m/s.

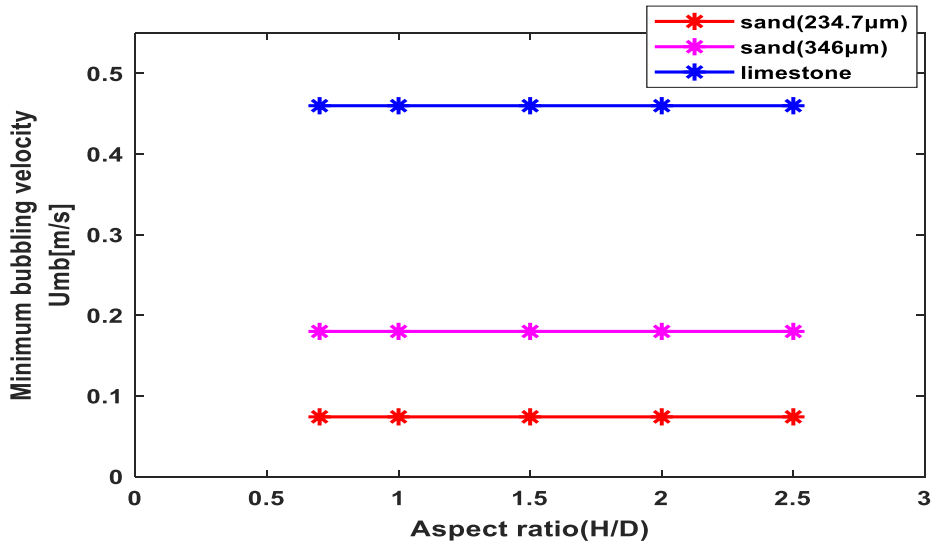

Figure 7.2: Variation in minimum bubbling velocity with change in static bed height

7.1.3 Minimum slug velocity

Figure 7.3. shows minimum slugging velocity of sand particle ($d_m = 234\mu m$) with different aspect ratios obtained from the experimental data and CPFD model. It can be seen that U_{ms} from the experiments and from the simulations are good in agreement. Also, two different correlations are used to predict U_{ms} for all aspect ratios and are compared with experimental and simulation results. Minimum slugging velocity correlations, as proposed by Agu et al.[22] and Baeyens and Geldart et al.[21], are used in this study. Since the particle size is relatively small, a round shape with sphericity 0.85 is used in the Agu et al. correlation. For $(h/D) < 1.5$, the Baeyens and Geldart et al. correlation under predict the minimum slugging velocity, while the Agu et al. correlation shows better agreement with experimental data for all aspect ratio

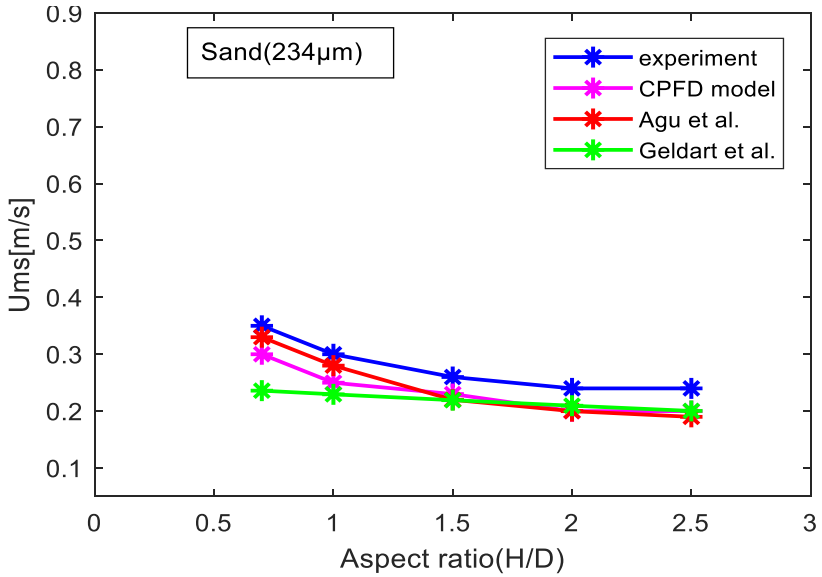

Figure 7.3: Minimum slugging velocity for sand particle

The minimum slugging velocity of sand particle ($d_m = 346\mu m$) and limestone ($d_m = 672\mu m$) are shown in Figure 7.6 and Figure 7.5 respectively. Minimum slugging velocity identified from the experimental and simulation data are compared with the correlations. It is observed that the CPFD model gives higher minimum slugging velocity than the experimental results. Baeyens and Geldart et al. correlation underpredicted U_{ms} value for sand particle below aspect ratio 1.5 while it over predict the U_{ms} above aspect ratio 1.5. With limestone, Baeyens and Geldart et al. over predict U_{ms} at aspect ratio greater than 1.5 as shown in Figure 7.5. In both case, sand and limestone, Agu et al correlation seems to predict the U_{ms} close to experimental value.

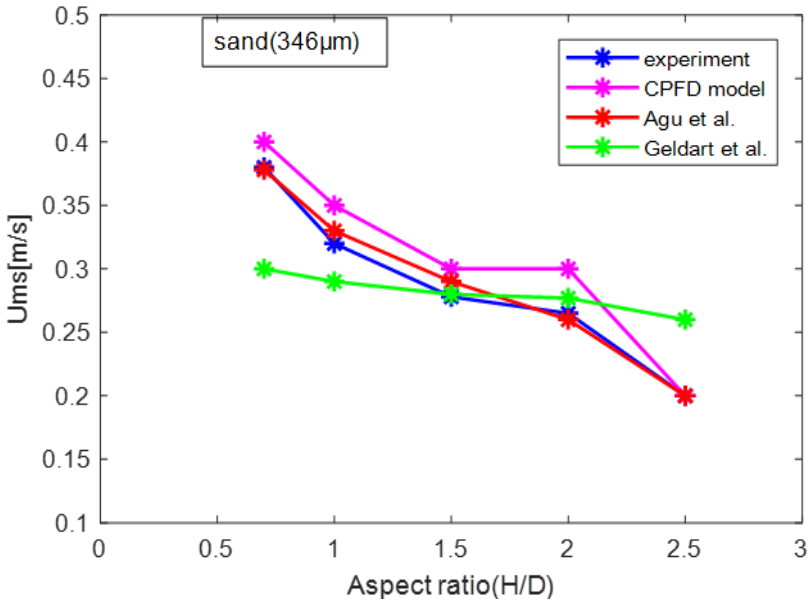

Figure 7.4: Variation of minimum slugging velocity for sand particles(346µm) with different static bed heights compared with experimental data, CPFD model and different correlations

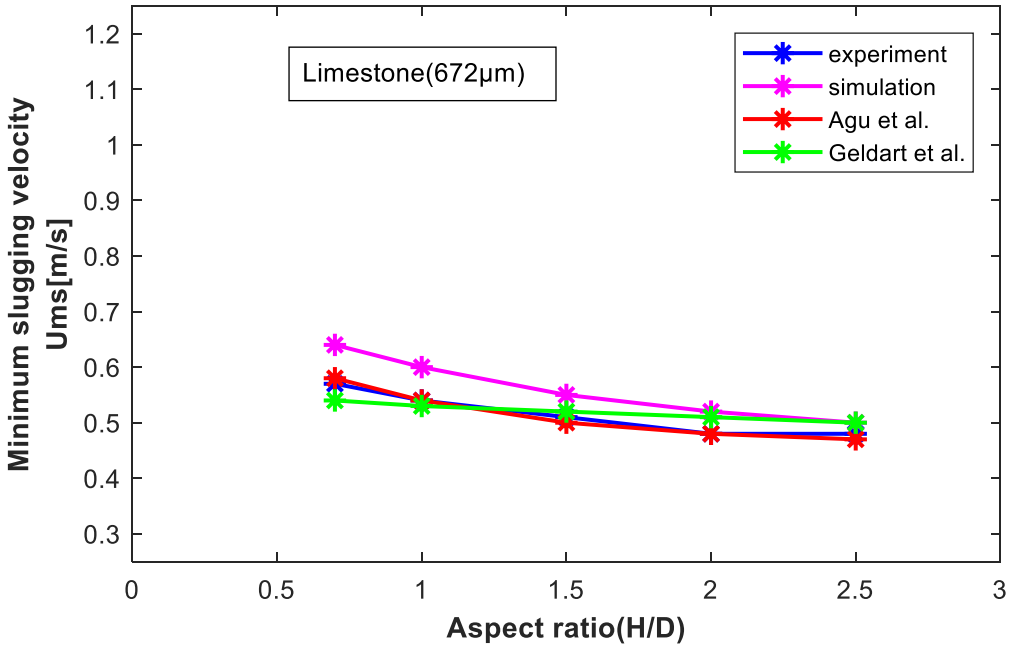

Figure 7.5: Variation of minimum slugging velocity for limestone with different static bed heights compared with experimental data, CPFD model and different correlations

The minimum slugging velocity obtained from the experimental data for sand particles and limestone, are compared in Figure 7.6. As can be seen from the figure, U_{ms} decreases with increase in aspect ratio for all the three types of particles. There is a slight increment in minimum slugging velocity with increase in mean diameter for sand particle. For limestone, the minimum slugging velocity seems to be established at significantly higher superficial gas velocity compared to the sand particles. This is due to increased density and mean diameter of the limestone

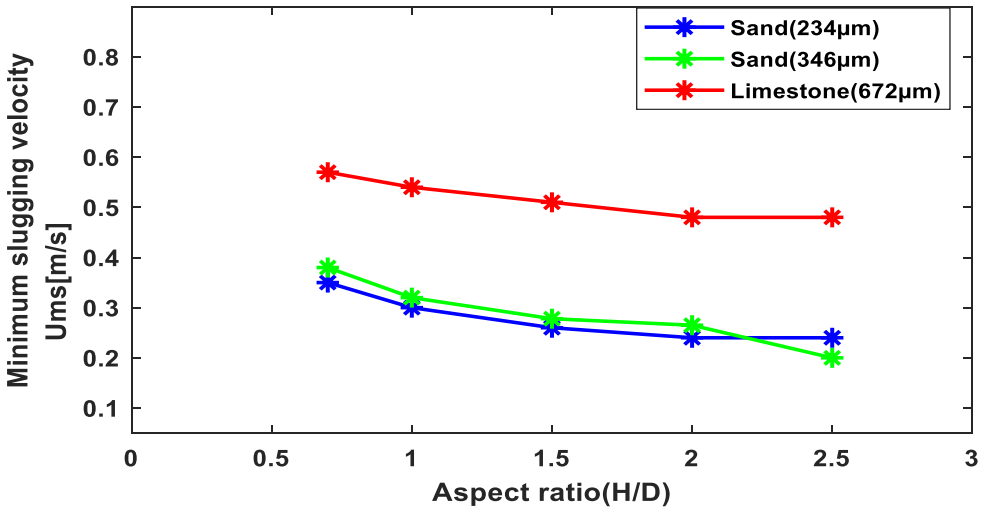

Figure 7.6: Minimum slugging velocity obtained from experimental data for three particles

7.1.4 Minimum turbulent velocity

7 shows minimum superficial gas velocity at which turbulent regime is established at different aspect ratio. The turbulent regime is identified using results obtained from the CPFD model for the three powders. It can be seen from the figure that with the increase in particle mean diameter there is a slight increment in minimum turbulent velocity. With the case of limestone, there is significant increase in superficial gas velocity at which the bed is fluidized as compared to sand particle. Similarly, for limestone and sand ($d_m = 346\mu m$), U_C remains constant with increase in aspect ratio below 1.5 and decreases with further increase in bed height.

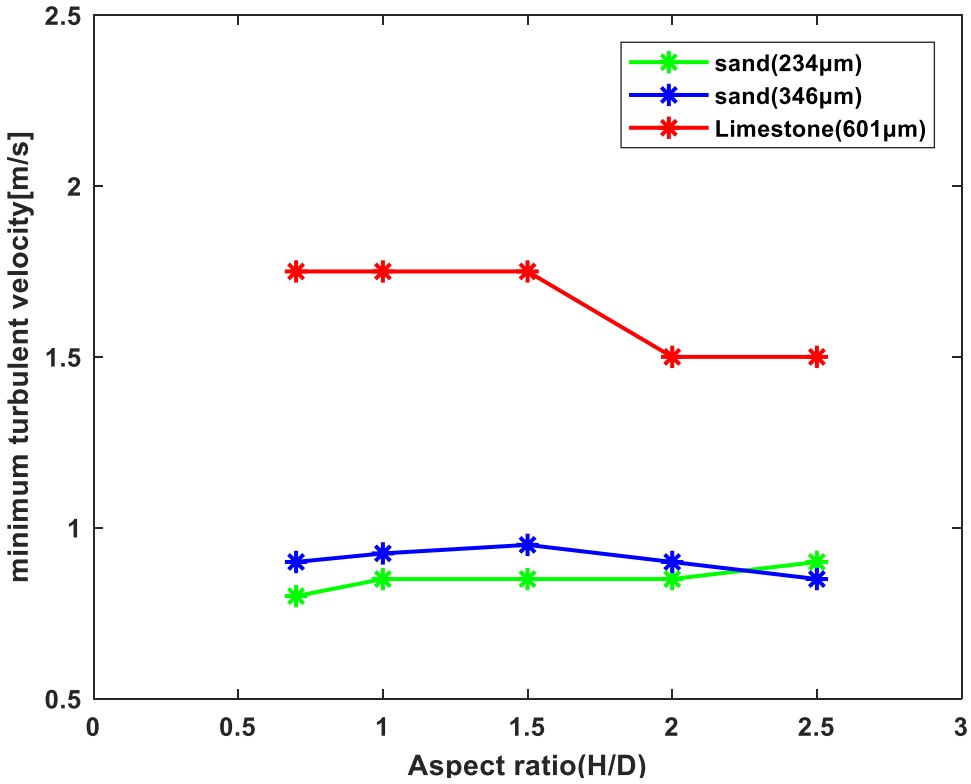

Figure 7.7:Minimum turbulent obtained from the simulation for three particles

Figure 7. shows minimum turbulent velocity for sand particle with mean diameter 234 μm. The minimum turbulent velocity obtained from the CPFD model is compared with the Bi and Grace et al. model proposed for turbulent velocity. The results show that the Bi et al. model predicts higher critical velocity compared to the CPFD model. The minimum turbulent velocity obtained from the CPFD model seems to increase with increasing static bed height. The Bi et al. model predicts a critical velocity that is higher than in the simulation and independent of the static bed height. The minimum turbulent velocity for limestone is shown in Figure 7.9. The U_C value obtained from the CPFD model, in the case of limestone, is higher up to an aspect ratio of 1.5 than that of the Bi et al. model and it reaches the same value for aspect ratio 2 and 2.5.

In case of sand with mean diameter $346\mu m$, the minimum turbulent velocity is independent of the static bed heights except for aspect ratio 0.7. The minimum turbulent velocity for sand ($d_m = 346\mu m$) is shown in Figure 7.1010.

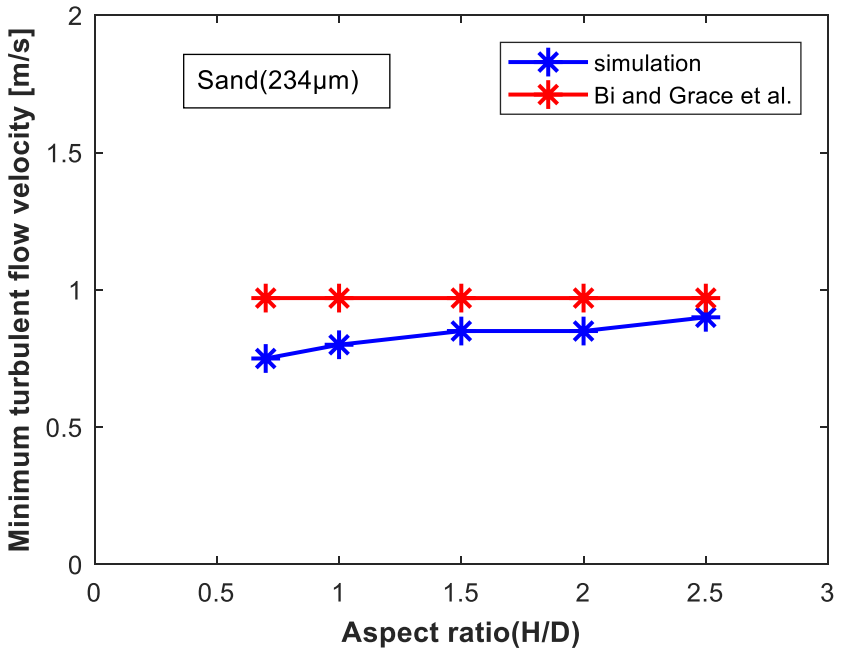

Figure 7.8:Minimum turbulent velocity of sand particle with different aspect ratio

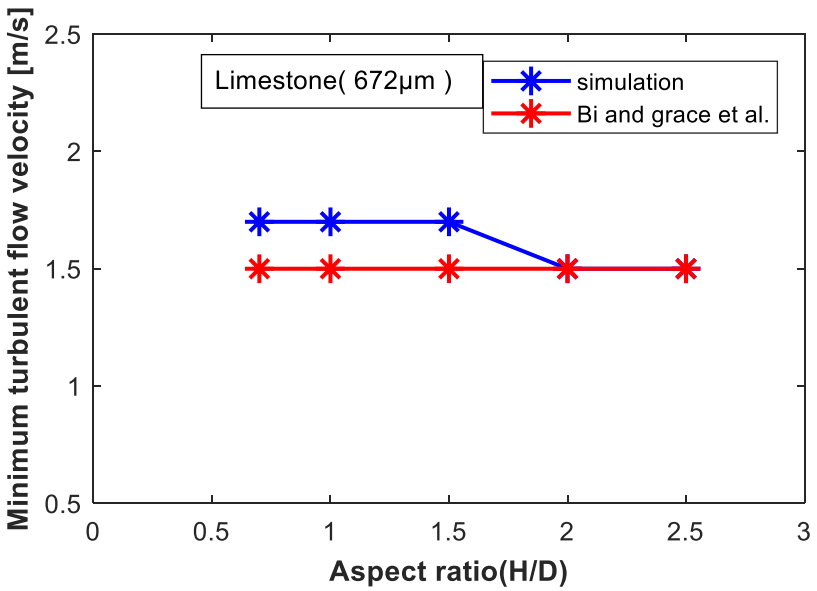

Figure 7.9:Minimum turbulent velocity of limestone at different aspect ratio

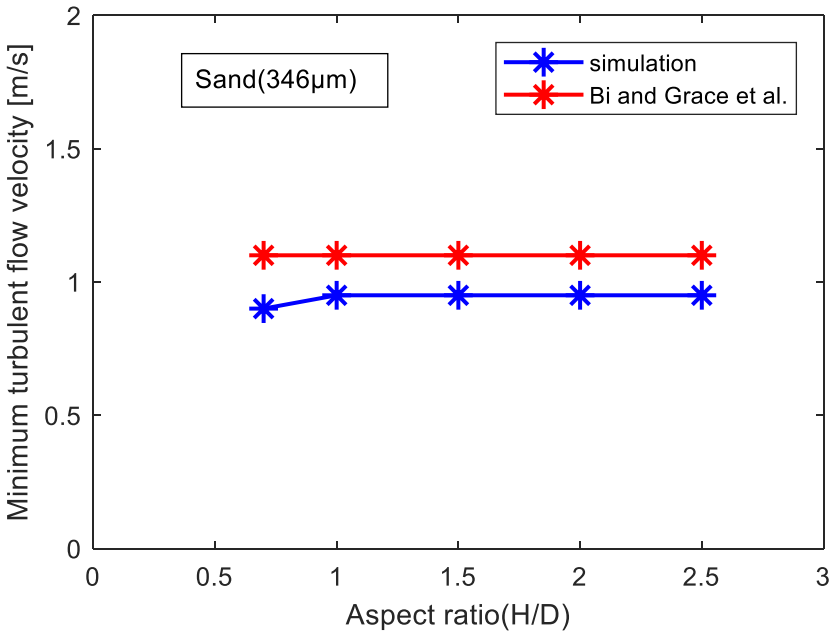

Figure 7.10:Minimum turbulent velocity of sand particle ($d_m = 346\mu m$) at different aspect ratio

8 Conclusion

Fluidized bed operations are usually carried out within a given flow regime. Fluidized bed regimes include particulate regime, bubbling regime, slugging regime and turbulent flow regime. This study investigates the effect of particle size, density and static bed height on the onset of different regime or transition of one regime to another.

Experiments were carried out on a cold fluidized bed with sand, limestone and glass beads particles with five different bed height/ bed diameter aspect ratios: 0.7, 1, 1.5, 2 and 2.5. Particles used in this work were selected based on criteria particle size, density and particle size distribution. The particles were sieved to identify the particle size distribution and the mean diameter. Further, a CPFD model was established using CPFD software Barracuda VR. A valid CPFD model was developed by comparing experimental data with simulation results obtained using different drag model and grid geometry. Since, a CPFD model using the Wen-Yu and Ergun drag model predicted the best results compared to experimental data, this model was used in this work. The data obtained from the experiments and simulations were used to establish and analyse different fluidization regimes. The minimum fluidization velocity for each type of particles and the aspect ratio were identified at the point of maximum pressure drop as a function of superficial gas velocity.

The U_{mf} for limestone with mean diameter $672\mu m$ and density $2837\ kg/m^3$ was found to be highest, $0.38\,m/s$, compared to sand and glass beads. Similarly, the other regimes: bubbling, slugging and turbulent regimes are estimated via standard deviation of pressure fluctuation as a function of superficial gas velocity.

The results show that the minimum fluidization velocity for limestone and sand particle ($d_m = 346\mu m$) remain constant with change in aspect ratio. However, for sand particle with mean diameter $234\mu m$, U_{mf} decreases when the aspect ratio is lower than 1.5. The minimum bubbling velocities for all the three types of particles are found to be independent of the static bed height. The results are obtained from the CPFD model for minimum slugging velocities are in good agreement with the experimental results and the trend is that U_{ms} decreases with increase in static bed height for all the three particle types. With the increase in the range of particle sizes for limestone, U_{ms} is found to increase significantly. Similarly, when comparing U_{ms} obtained from the experiments and the CPFD code with two different correlation proposed by Agu et al. and Bayens and Geldart et al., it was found that the Agu correlation for minimum slugging velocity agrees well with the experimental results. Likewise, the onset of turbulent velocity was found to be independent of the static bed height as predicted by Bi et al. For sand particle ($d_m = 234\mu m$), the simulation results show that the U_C increases with increase is static bed height. While, for sand particle ($d_m = 346\mu m$) and limestone U_C almost remain constant with change in aspect ratio expect at the aspect ratio of 1.5 (in the case of limestone) where it decreases to a stable value. Thus, it can be concluded that the methods applied to identify and analyse the different flow regimes in this work are satisfactory, when compared to different correlation.

References

[1] D. Kunii and O. Levenspiel, *Fluidization engineering*. Elsevier, 2013.

[2] T. S. Hargest and C. P. Artz, "A New Concept in Patient Care: The Air-Fluidized Bed," *AORN journal*, vol. 10, no. 3, pp. 50-53, 1969.

[3] R. Sarker, M. Rahman, N. Love, and A. Choudhuri, "Effect of Bed Height, Bed Diameter and Particle Shape on Minimum Fluidization in a Gas-Solid Fluidized Bed," in *50th AIAA Aerospace Sciences Meeting including the New Horizons Forum and Aerospace Exposition*, 2012, p. 644.

[4] D. Escudero and T. J. Heindel, "Bed height and material density effects on fluidized bed hydrodynamics," *Chemical Engineering Science*, vol. 66, no. 16, pp. 3648-3655, 2011.

[5] C. A. S. Felipe and S. C. S. Rocha, "Prediction of minimum fluidization velocity of gas–solid fluidized beds by pressure fluctuation measurements — Analysis of the standard deviation methodology," *Powder Technology*, vol. 174, no. 3, pp. 104-113, 2007/05/25/ 2007.

[6] A. R. Abrahamsen and D. Geldart, "Behaviour of gas-fluidized beds of fine powders part I. Homogeneous expansion," *Powder technology*, vol. 26, no. 1, pp. 35-46, 1980.

[7] J. S. Dennis, "3 - Properties of stationary (bubbling) fluidised beds relevant to combustion and gasification systems A2 - Scala, Fabrizio," in *Fluidized Bed Technologies for Near-Zero Emission Combustion and Gasification*: Woodhead Publishing, 2013, pp. 77-148e.

[8] W. Bauer, J. Werther, and G. Emig, "Influence of gas distributor design on the performance of fluidized bed reactor," *Ger. Chem. Eng*, vol. 4, pp. 291-298, 1981.

[9] J. Yates, *Fundamentals of Fluidized-Bed Chemical Processes: Butterworths Monographs in Chemical Engineering*. Butterworth-Heinemann, 2013.

[10] J. Yerushalmi and N. T. Cankurt, "Further studies of the regimes of fluidization," *Powder Technology*, vol. 24, no. 2, pp. 187-205, 1979/11/01/ 1979.

[11] C. Vial, E. Camarasa, S. Poncin, G. Wild, N. Midoux, and J. Bouillard, "Study of hydrodynamic behaviour in bubble columns and external loop airlift reactors through analysis of pressure fluctuations," *Chemical Engineering Science*, vol. 55, no. 15, pp. 2957-2973, 2000/08/01/ 2000.

[12] S. Ergun and A. A. Orning, "Fluid Flow through Randomly Packed Columns and Fluidized Beds," *Industrial & Engineering Chemistry*, vol. 41, no. 6, pp. 1179-1184, 1949/06/01 1949.

[13] A. Anantharaman, R. A. Cocco, and J. W. Chew, "Evaluation of correlations for minimum fluidization velocity (Umf) in gas-solid fluidization," *Powder Technology*, vol. 323, pp. 454-485, 2018/01/01/ 2018.

[14] H. M. Jena, G. K. Roy, and K. C. Biswal, "Studies on pressure drop and minimum fluidization velocity of gas–solid fluidization of homogeneous well-mixed ternary mixtures in un-promoted and promoted square bed," *Chemical Engineering Journal*, vol. 145, no. 1, pp. 16-24, 2008/12/01/ 2008.

[15] P. Bourgeois and P. Grenier, "The ratio of terminal velocity to minimum fluidising velocity for spherical particles," *The Canadian Journal of Chemical Engineering*, vol. 46, no. 5, pp. 325-328, 1968.

[16] S. Babu, B. Shah, and A. Talwalkar, "Fluidization correlations for coal gasification materials-minimum fluidization velocity and fluidized bed expansion ratio," in *AIChE Symp. Ser*, 1978, vol. 74, no. 176, pp. 176-186.

[17] K. Hillegardt and J. Werther, "Local bubble gas hold-up and expansion of gas/solid fluidized beds," *German chemical engineering*, vol. 9, no. 4, pp. 215-221, 1986.

[18] J. Davidson, D. Harrison, and R. Jackson, "Fluidized particles: Cambridge University Press, 1963. 155 pp. 35s," ed: Pergamon, 1964.

[19] V. Rudolph and M. Judd, "Circulation and slugging in a fluid bed gasifier fitted with a draft tube," in *Circulating Fluidized Bed Technology: Proceedings of the First International Conference*, 1986, pp. 437-442: Elsevier.

[20] P. S. B. Stewart and J. F. Davidson, "Slug flow in fluidised beds," *Powder Technology*, vol. 1, no. 2, pp. 61-80, 1967/06/01/ 1967.

[21] J. Baeyens and D. Geldart, "An investigation into slugging fluidized beds," *Chemical Engineering Science*, vol. 29, no. 1, pp. 255-265, 1974.

[22] C. E. Agu, C. Pfeifer, M. Eikeland, L.-A. Tokheim, and B. M. E. Moldestad, "Models for Predicting Average Bubble Diameter and Volumetric Bubble Flux in Deep Fluidized Beds," *Industrial & Engineering Chemistry Research*, vol. 57, no. 7, pp. 2658-2669, 2018/02/21 2018.

[23] M. Horio and K. Morishita, *Flow Regimes of High Velocity Fluidization*. 1988, pp. 117-136.

[24] H. T. Bi, N. Ellis, I. A. Abba, and J. R. Grace, "A state-of-the-art review of gas–solid turbulent fluidization," *Chemical Engineering Science*, vol. 55, no. 21, pp. 4789-4825, 2000/11/01/ 2000.

[25] M. PunČOchÁŘ, J. DrahoŠ, J. ČErmÁK, and K. SeluckÝ, "EVALUATION OF MINIMUM FLUIDIZING VELOCITY IN GAS FLUIDIZED BED FROM PRESSURE FLUCTUATIONS*," *Chemical Engineering Communications*, vol. 35, no. 1-6, pp. 81-87, 1985/05/01 1985.

[26] S. Hong, B. Jo, D. Doh, and C. Choi, "Determination of minimum fluidization velocity by the statistical analysis of pressure fluctuations in a gas—solid fluidized bed," *Powder Technology*, vol. 60, no. 3, pp. 215-221, 1990.

[27] Y. O. Chong, D. P. O'Dea, E. T. White, P. L. Lee, and L. S. Leung, "Control of the quality of fluidization in a tall bed using the variance of pressure fluctuations," *Powder Technology*, vol. 53, no. 3, pp. 237-246, 1987/12/15/ 1987.

[28] B. Gourich, C. Vial, A. H. Essadki, F. Allam, M. Belhaj Soulami, and M. Ziyad, "Identification of flow regimes and transition points in a bubble column through analysis of differential pressure signal—Influence of the coalescence behavior of the liquid phase," *Chemical Engineering and Processing: Process Intensification*, vol. 45, no. 3, pp. 214-223, 2006/03/01/ 2006.

[29] W. Tchowa Medjiade, A. Rosenbaum Alvaro, and A. Schumpe, "Flow regime transitions in a bubble column," *Chemical Engineering Science*, vol. 170, pp. 263-269, 2017/10/12/ 2017.

Appendices

Appendix A

Regime Identification

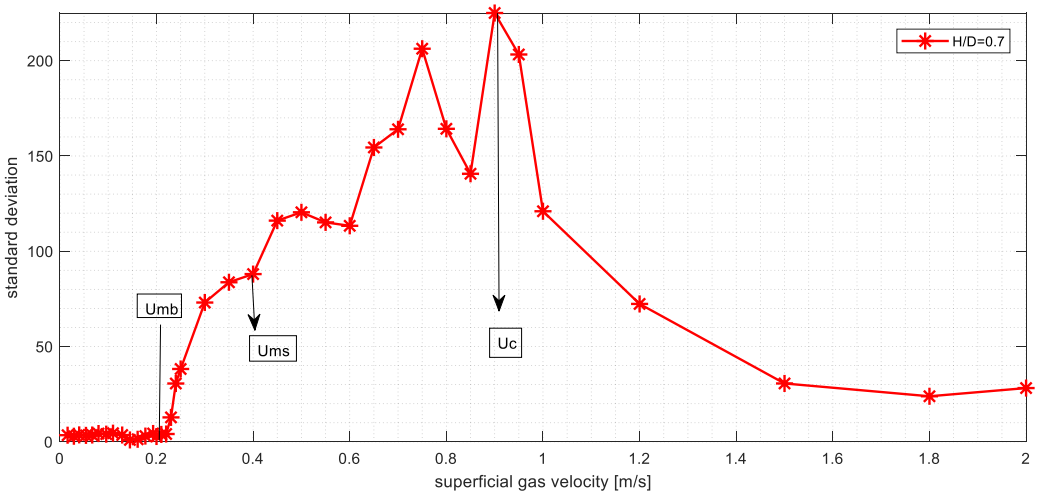

Pressure drop fluctuation showing onset of different regimes for sand particles

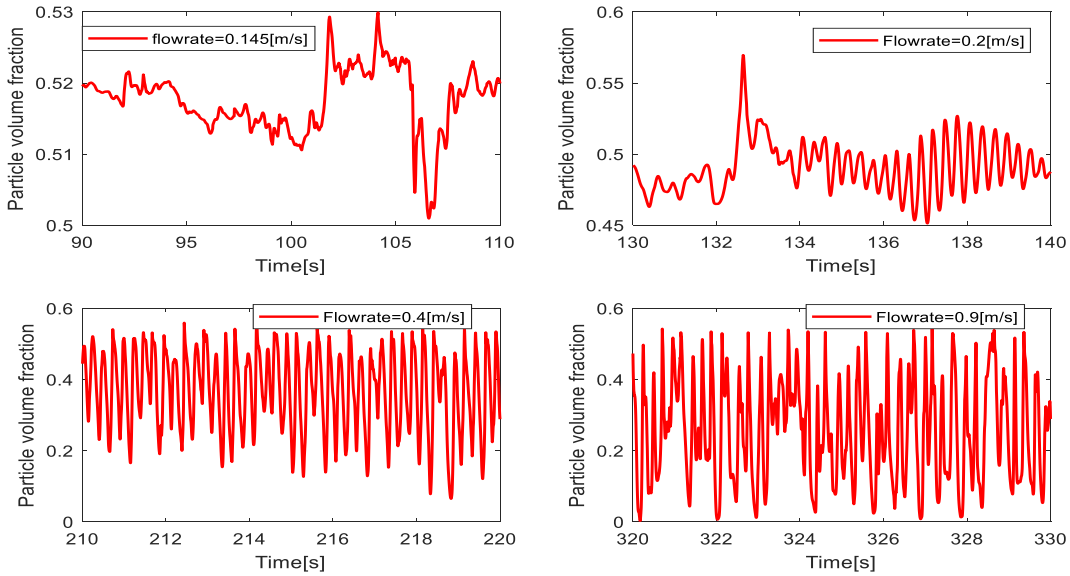

Change in solid volume fraction at the onset of different fluidization regime, minimum fluidization, minimum bubbling regime, minimum slugging regime minimum turbulent regime

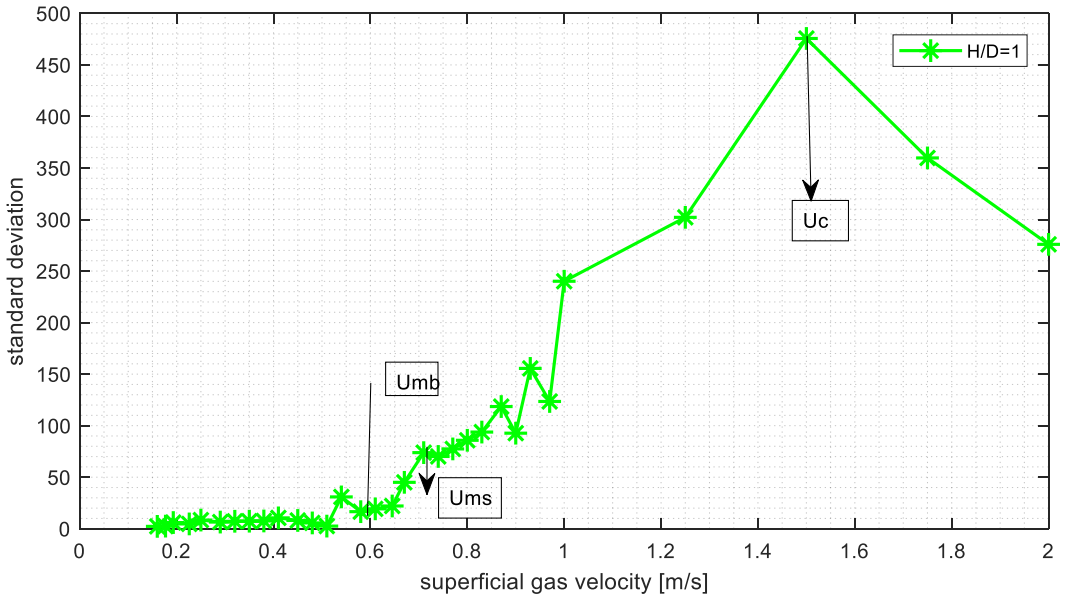

Pressure drop fluctuation showing onset of different regimes for limestone

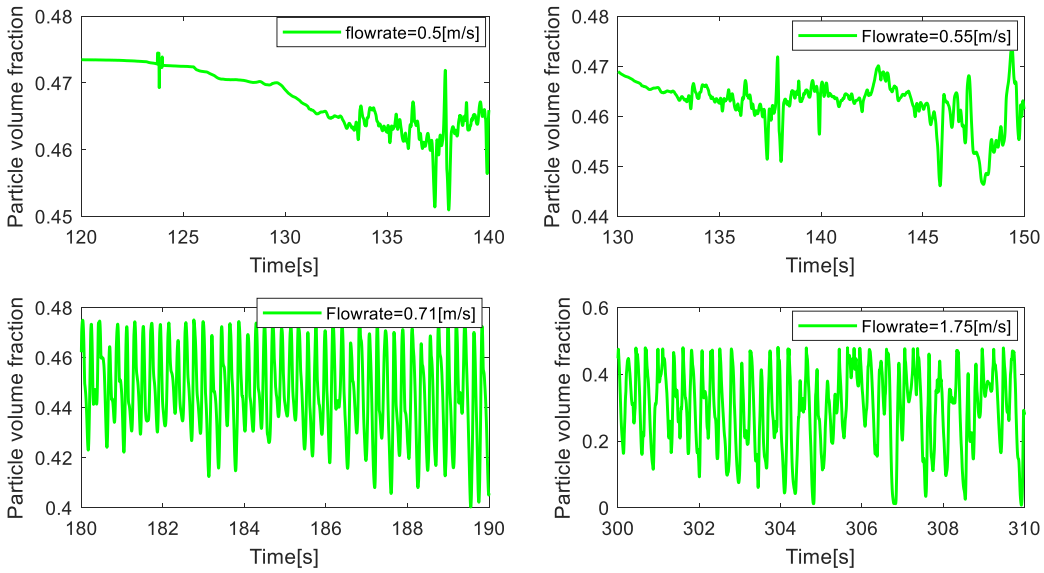

Change in solid volume fraction at the onset of different fluidization regime, minimum fluidization, minimum bubbling regime, minimum slugging regime minimum turbulent regime

Appendix B

Code

```
close all;
clear;
clc;

%Reading file
%%
data = dlmread('sand_200_400_2.5.txt');
avgData = zeros(1,8);
stdData=0;
ul=380;
ll=0;
dt=10;
n=380/10;
for i=1:n
    [indices] = Indices(data, 1, dt*i-2 ,i*dt);%first column(indices to be checked) including 10
    tempData = data(indices, 2:end);
    avgData = [avgData;mean(tempData)];
     data2=tempData(:,1)-tempData(:,3);
     stdData=[stdData;std(data2)];
end

averagedata=avgData(2:end,:);
stdData=stdData(2:end,:);
dp=averagedata(:,1)-averagedata(:,6);
Q=[0.016,0.029,0.04,0.054,0.067,0.08,0.096,0.11,0.129,0.145,0.161,0.177,0.193,0.2:0.01:0.2
5,0.3:0.05:1,1.2,1.5,1.8,2]';
dataMatrix = ([Q, dp]);
%Plot
%%
figure
plot(Q, dp,'O-R','LineWidth', 1.5, 'MarkerSize',10);
legend('H/D=2');
title('Pressure drop vs superficial gas velocity');
xlabel('Superficial gas velocity [m/s]')
ylabel('pressure drop [Pa]')
grid('minor')
axis([0 0.4 0 3500])
set(gca, 'FontSize', 10,'FontWeight','Bold')
%%
figure, plot(Q, stdData,'*-r','LineWidth', 1.5, 'MarkerSize',10)
legend('H/D=2');
xlabel('superficial gas velocity [m/s]')
ylabel('standard deviation')
grid('minor')
set(gca, 'FontSize', 28,'FontWeight','Bold')
```

```
axis([0 0.2 -inf inf]);
axis([0 inf 0 inf]);


%subplot
%%
subplot(2,2,1);
for j=1:n
   [indices] = Indices(data, 1, 90 ,110);
   data3=data(indices,1:9);
end
plot(data3(:,1),data3(:,8),'r','lineWidth',1.5);
legend('flowrate=0.145[m/s]')
xlabel('Time[s]')
ylabel('Particle volume  fraction')


subplot(2,2,2);
for j=1:n
   [indices] = Indices(data, 1, 130 ,140);
   data3=data(indices,1:9);
end
plot(data3(:,1),data3(:,8),'r','lineWidth',1.5);
legend('Flowrate=0.2[m/s]')
xlabel('Time[s]')
ylabel('Particle volume  fraction')


subplot(2,2,3);
for j=1:n
   [indices] = Indices(data, 1,210,220);
   data3=data(indices,1:9);
end
plot(data3(:,1),data3(:,8),'r','lineWidth',1.5);
legend('Flowrate=0.4[m/s]')
xlabel('Time[s]')
ylabel('Particle volume  fraction')


subplot (2,2,4);
for j=1:n
   [indices] = Indices (data, 1, 320 ,330);
   data3=data(indices,1:9);
end
plot(data3(:,1),data3(:,8),'r','lineWidth',1.5);
legend('Flowrate=0.95[m/s]')
xlabel('Time[s]')
ylabel('Particle volume  fraction')
```

Indices based code

```
function [indices] = Indices(data, columnBase, LL, UL)
indices1 = data(:,columnBase)>LL;
indices2 = data(:,columnBase)<=UL;
indices = indices1+indices2>1;
end
```